

1 **Climate change effects on groundwater recharge in Yucatan Peninsula.**

2 **Application of water balance models to GCMs**

3

4 Edgar Rodríguez-Huerta^a, *, Martí Rosas-Casals^{a,b} and Laura Margarita Hernández
5 Terrones^c

6 ^a *Sustainability Measurement and Modeling Lab (SUMMLab), Universitat Politècnica de
7 Catalunya (UPC – BarcelonaTech), ESEIAAT, Campus Terrassa, 08222 Barcelona, Spain;* ^b *Institute for Sustainability Science and Technology (IS.UPC), Universitat Politècnica de
9 Catalunya (UPC – Barcelona Tech), Campus Diagonal Nord, 08034 Barcelona, Spain;* ^c *Universidad del Caribe, L-1. Mz 1, Esq. Fracc. Tabachines SM 78, 77528, Cancún Quintana
11 Roo, México*

12 * Corresponding author: edgar.rodriguez@upc.edu

13

14 **Abstract:**

15 The effects of climate change are significant on groundwater recharge. In regions with
16 socioeconomic structures highly dependent on this kind of water source, expected positive
17 and negative variations in temperature and precipitation respectively, will have a negative
18 effect on the recharge of groundwater and, consequently, on the future well-being of their
19 inhabitants. In this paper we aim at estimating the effect that changes in climatic
20 parameters will have on groundwater recharge in one of these areas: the Yucatan Peninsula
21 (Mexico). We apply a monthly water balance model to five distinct Global Circulation
22 Models in the near horizon (2015-2039), with RCP 4.5 and 8.5. In average terms, our
23 results estimate a current recharge between 118 ± 33 mm per year, which represents around
24 10 % of the total annual precipitation, and a reduction of 23% of groundwater recharge, a
25 result which clearly threatens the future socioecological equilibrium of the region.

26 Keywords: Climate change; Groundwater recharge; Yucatan Peninsula; Monthly water
27 balance model

28 **1. Introduction**

29 The effects on climate change are already perceptible in many places around the world,
30 with changes in precipitation (temporal distribution and intensity) (Dore, 2005; Gao et al., 2018;
31 Madsen et al., 2014; Trenberth, 2011), increasing and more threatening periods of drought (Dale
32 et al., 2001, Magaña *et al.*, 1999, Mulholland *et al.*, 1997), and with a generalized increase in
33 temperatures (Jauregui, 2005, Liverman & O'Brien, 1991, Schär *et al.*, 2004). This rise in the
34 global temperature causes at the same time an increase in potential evapotranspiration which,
35 combined with rainfall variations, can modify the hydrological cycle of any region (Findlay,
36 2003, Green *et al.*, 2011, R. G. Taylor *et al.*, 2013). All these factors, combined with the effects
37 caused by the growth and development of societies (i.e. modifications in water flows and water
38 supply, transformation of the stream network, changes in runoff characteristics, land use,
39 deforestation and urbanization) (Grobick, 2010, Savenije *et al.*, 2014), are causing significant
40 alterations in the water balance, and negative effects in water availability (Bates *et al.*, 2008,
41 Milly *et al.*, 2005). In the particular case of coastal regions with socioeconomic activities mostly
42 based on tourism and/or the tertiary sector, and highly dependent on groundwater sources and
43 recharge (Pulido-Velazquez, Renau-Pruñonosa, *et al.*, 2018), modifications in water flows and
44 supply, together with changes in runoff characteristics and salinity in coastal aquifers, make
45 alterations in the water balance much more critical (Aranda-Cirerol *et al.*, 2010, Marin & Perry,
46 1994). For these reasons, assessing and quantifying the potential impact of climate change on
47 water resources is an imperative task, especially for those regions with a generalized lack of
48 bioclimatic data like the Yucatan Peninsula, in Mexico.

49 The IPCC Fourth Assessment Report (IPCC, 2007) identified a knowledge gap
50 concerning the impact of climate change on groundwater resources, and how it affects
51 hydrogeological processes in both direct and indirect ways. Since then, different studies have
52 been carried out to analyze the relationship between, and variables involved in, climate change
53 and groundwater recharge. For example, Green et al. (2011), Kløve et al. (2014), Meixner et al.
54 (2016), Smerdon (2017), Taylor et al. (2013), (Holman *et al.*, 2012) compiled key factors and
55 described the effects of climate change on groundwater and dependent ecosystems. Ali et al.
56 (2012) used climatic data from global circulation models (GCM) (D. M. Allen *et al.*, 2010,
57 Huebener *et al.*, 2007, IPCC, 2013, Pulido-Velazquez, Collados-Lara, *et al.*, 2018, von Storch *et*
58 *al.*, 1993) to project the effects of climate change on specific regions. Herrera-Pantoja and
59 Hiscock (2008) applied a methodology based on a model of soil moisture balance, with a daily
60 data generator to project the repercussions in recharge.

61 Here we aim at assessing the water balance of the hydrological region XII (CONAGUA
62 & SEMARNAT, 2012) located in Yucatan Peninsula (YP) to determine the possible effects that
63 climate change will have on the groundwater recharge. We consider different methods for the
64 estimation of the potential evapotranspiration, and we include the effect of land uses and land
65 cover (LULC) in the soil moisture storage capacity to analyze their influence in the variability of
66 groundwater recharge. No similar analysis has been found for this same region and scale in the
67 literature. The effects of climate change are analyzed using climatic data from GCM as input
68 parameters in several groundwater recharge scenarios, and considering the variations in
69 precipitation and temperature. Knowing these potential changes, will allow making a better
70 planning of resources, generating more awareness in future allocations of water use and
71 establishing new extraction limits that guarantee a sustainable water use in the YP.

72 Another contribution is to generate a tool for visualizing results (section 4.1), which
73 allows the user (decision makers) to make personalized analyzes in different subregions, and
74 choose different GCMs to visualize their effects on vertical recharge in the Yucatan Peninsula.

75 **2. Materials and methods**

76 In this section we present, firstly, the groundwater characteristics description of the
77 region; secondly, the water balance model, including information about precipitation,
78 temperature, soil moisture storage capacity and sub-models for evapotranspiration. Finally, we
79 describe the processes of (1) combining water balance and climate change models and (2)
80 adapting to a reduction of scale for the region.

81 ***2.1. Groundwater characteristics in Yucatan Peninsula***

82 In 2010, 13 hydrological-administrative regions were defined by The National Water
83 Commission of Mexico (CONAGUA), being the Yucatan Peninsula the Hydrological-
84 Administrative Region XII (RHA-XII-PY) (CONAGUA, 2016). It includes the states of
85 Yucatan, Quintana Roo, and Campeche. It is located in the southeastern part of Mexico and it
86 has a territorial extension of 139,897 km² (CONAGUA, 2015a). The main source of water in the
87 YP is groundwater, due to its topological and geological characteristics –karstic platform with
88 dolomites, limestones, and evaporites—, surface-water runoff and drainage are practically non-
89 existent, with the exception of some southern parts of the Peninsula (Campeche and Quintana
90 Roo) (CONAGUA, 2015a) (Gondwe *et al.*, 2010), whereby rainwater evaporates, it's absorbed
91 by plants, soil and infiltrates to the subsoil (Estrada Medina & Cobos Gasca, 2012).

92 Additionally, the high groundwater level and the lack of soil, make the solutes infiltrate to the
93 groundwater, making it vulnerable to contamination (Aranda-Cirerol *et al.*, 2010, Pérez Ceballos
94 & Pacheco Ávila, 2004).

95 The high rainfall (CONAGUA, 2015a, INEGI, 2015), the great infiltration capacity of the
96 karstic rock, and the reduced topographic slope favors the renewal of the YP groundwater, so
97 practically the whole area behaves as a recharge zone (Bauer-Gottwein *et al.*, 2011, Holliday *et*
98 *al.*, 2007). However, although the aquifer receives abundant recharge, deforestation and climate
99 change effects in the region (i.e., less precipitation and temperature increase), suggest that the
100 recharge will be diminished in the next years (Alan *et al.*, 2015, Sánchez Aguilar & Rebollar
101 Domínguez, 1999).

102 Scientific research studies have been carried out in the region in order to establish the
103 groundwater recharge volume for the following purposes essentially (Table 1): (a) to describe
104 the hydrological functioning of the area (Bauer-Gottwein *et al.*, 2011, INEGI, 2002, Lesser,
105 1976, SEMARNAT, 2015, Villasuso & Méndez, 2000), (b) to establish the permissible limits for
106 water extraction and supply (CONAGUA, 2015b), (c) to analyze the vulnerability of water
107 resources (Beth I. Albornoz-Euán, 2007, Pérez Ceballos & Pacheco Ávila, 2004, Torres *et al.*,
108 2014), and (d) to characterize the groundwater flows that exist in the region (González-Herrera *et*
109 *al.*, 2002).

110 Table 1. Summary of YP recharge studies. (P , precipitation, ET_a , actual evapotranspiration, R ,
111 recharge, NA , not available/specified)

Autor	method	P (mm)	ET _a (mm)	R (mm)	Area
Lesser (1976)	Turc (1961)	1050	900	150	YP
Hanshaw and Back (1980)	NA	NA	NA	150	YP
Villasuso (2000)	Thornthwaite (1948)	1300	1060	240	YP
González-Herrera (2002)	AQUIFER model (1991)	1300	NA	233	Yucatan
INEGI (2002)	NA	1135	900	230	Yucatan
Pérez and Pacheco (2004)	NA	NA	NA	110 - 300	Yucatan

Albornoz Euan (2007)	Turc (1961)	1200 - 1500	600 - 800	0 - 491	Yucatan
Gondwe et al. (2010)	Priestley– Taylor equation (1972)	1260	960	290	YP
Torres Díaz, M.C. (2014)	NA	NA	NA	198 - 276	North and center of Yucatan
SEMARNAT (2015)	Penman (1948)	1070	NA	182	YP
CONAGUA (2015b)	NA	1100 - 1430	1236	146	YP
Carballo Parra (2016)	Hargreaves (1985)	1200	NA	220 - 360	Quintana Roo

112

113 Complementary, studies on climate change impacts in the region have focused in relevant
 114 aspects, like changes on bioclimatic parameters description (Orellana *et al.*, 2009), or the
 115 analysis of the vulnerability index of the aquifer to polluting agents (Bethsua Iztaccihuatl
 116 Albornoz-Euán *et al.*, 2017). Nevertheless, a study about the effects of climate change on
 117 groundwater recharge in YP from a monthly water balance model, applied at a regional scale
 118 such as this study has not been found in the existing literature.

119 **2.2. Water-balance model for Yucatan Peninsula**

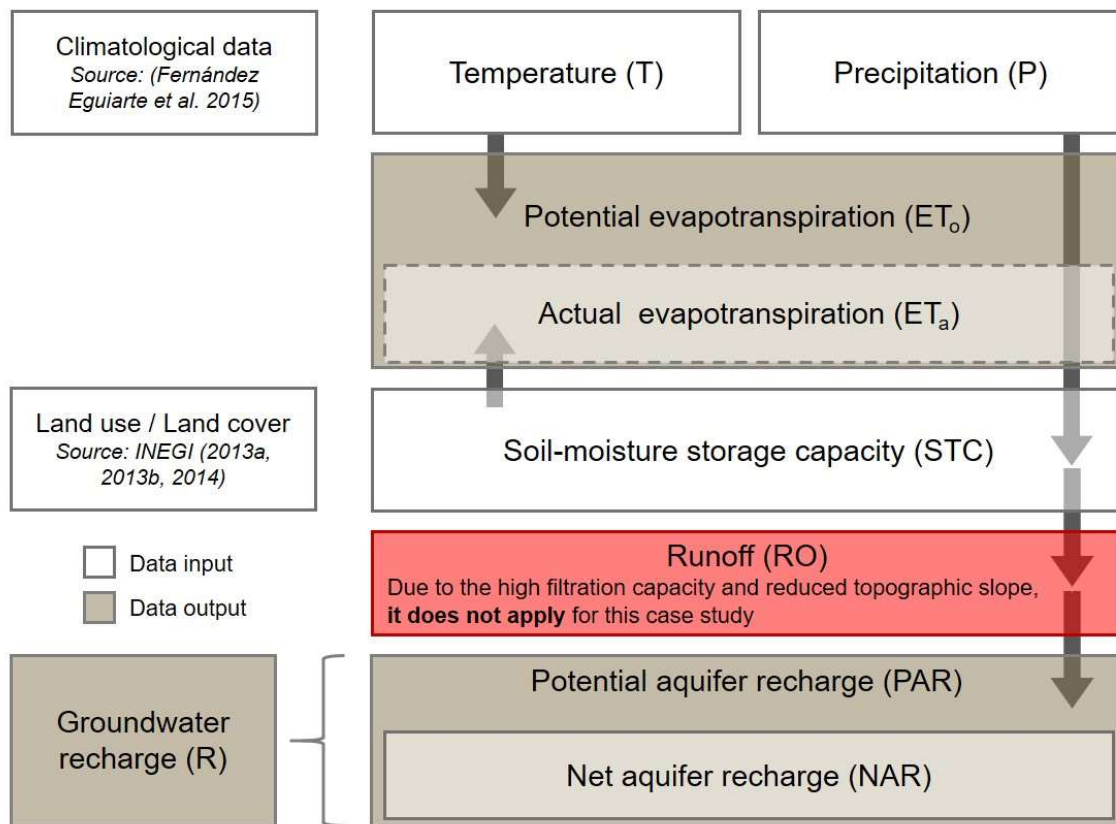
120 A water balance consists on the application of the mass conservation principle to a whole
 121 basin, or to a part of it, constrained by some boundary conditions, and during a period of time
 122 (Alley, 1984). The difference between the total of inputs and outputs must be equal to the storage
 123 variation (equation 1). When the unit of time is large, the variations in the stored volume are
 124 negligible and, in that case, inputs equal the outputs (Schulz & García, 2015).

125 $Inputs - Outputs = \Delta Storage$ (1)

126 The recharge of groundwater (R) can be explained following the precipitation path
 127 (Charles, 2003). An amount of the precipitation (P) is returned to the atmosphere through
 128 evapotranspiration. Actual evapotranspiration (ET_a) refers to water that returns to the atmosphere
 129 from vegetated areas by the evaporation of soil, plant surface, and soil, water absorbed by the
 130 plants roots and transpired through leaves. Water infiltrated into the soil that is not returned to
 131 the atmosphere by evapotranspiration moves vertically downwards, going into groundwater
 132 when it reaches the saturated zone (Figure 1). Surface runoff (RO) processes have not been

133 considered since they do not practically occur in the study area due to the high infiltration
134 capacity of karstic formations.

135 The groundwater recharge was establish as potential aquifer recharge (PAR) because we
136 consider that is all water which filtrate below the root zone (Pulido-Velazquez, Collados-Lara, *et*
137 *al.*, 2018, Rushton, 1988) and includes excess precipitation that exceeds the maximum of soil-
138 moisture storage capacity (STC) (de Vries & Simmers, 2002).



139 Figure 1. Water-balance model diagram. Adapted from (McCabe & Markstrom, 2007)

140

141 According to the physical conditions of the YP and the methodology for estimating the
142 monthly water balance, the following assumptions were considered:

- 143 • The entire surface works as a recharge area (Bauer-Gottwein *et al.*, 2011, Holliday *et al.*,
144 2007).
- 145 • Runoff is considered negligible given the reduced topographic slope and geology
146 characteristics (Beth I. Albornoz-Euán, 2007, Carballo Parra, 2016, Cervantes Martínez,
147 2007, Gondwe *et al.*, 2010).

- Groundwater recharge includes, but does not distinguish between, recharge to aquifers and non-aquifers.
- Our model only includes natural groundwater recharge, and dismiss withdrawals of groundwater.
- Changes in the parameters of land use change caused by human intervention, as well as the effects on soil cover, and vegetation patterns (Section 4.2) were omitted.

Recharge from surface water bodies and submarine groundwater discharge (SGD) (Null *et al.*, 2014) are discarded.¹ To calculate the recharge, we adapted the monthly water balance model developed by Thornthwaite (Thornthwaite, 1948, Thornthwaite & Mather, 1955, 1957) (equation 2). We consider model type *T* properties, described by Alley (1984). In this type of models, it is assumed that the soil has a specific soil-moisture storage capacity *STC*, and moisture is added or subtracted monthly, depending on whether the precipitation is greater or less than evapotranspiration, as long as it remains within the maximum capacity of soil moisture *SM* (Alley, 1984).

$$R = P - \Delta SM - ET_a \quad (2)$$

2.2.1. Precipitation and temperature

Our objective in the use of these specific climatological data is to compare the results of historical data with the different climate change scenarios of the Digital Climatic Atlas of Mexico (DCAM) (Fernandez-Eguiarte A., J. Zavala-Hidalgo., 2010, A Fernández Eguiarte *et al.*, 2015a) presented under the same format and spatial resolution. In addition, due to its very high spatial resolution, the deployment of the maps covers the national, state, municipal and regional scales.

Precipitation and temperature data were obtained by A Fernández Eguiarte *et al.* (2014, 2015a). Agustín Fernández Eguiarte et al. (2014) calculated bioclimatic parameters from a daily climatological database from the Mexican National Meteorological Service (SMN) and from year 1961 to year 2000. In this work, daily data from more than 5200 meteorological stations

¹ Surface water bodies and SGD occurs around the coast of the peninsula with estimated discharges between 23,500 m³ km² d⁻¹ (Hanshaw & Back, 1980) and 40,000 m³ km² d⁻¹ (Valle-Levinson *et al.*, 2011).

were processed to obtain monthly values for bioclimatic parameters for each one of the meteorological stations, considering only those stations with more than thirty years of records. Subsequently, they obtained the difference between monthly averages of each station, and the corresponding value in the average monthly climatic surface of the WorldClim-Global Climate Data base (1950-2000)² (Hijmans et al., 2005). From the set of differences, they eliminated the stations whose values were above or below 2 standard deviations in each corresponding month. Finally, they applied spatial interpolation of the remaining differences using inverse distance weighted method (IDW) (Lu & Wong, 2008) at very high resolution (926 m) according to the same methodology implemented by Hijmans et al. (2005), which was added to the reference surface of WorldClim-Global Climate Database. From these source data, in this paper we use monthly averages of maximum, minimum, and mean temperature, as well as accumulated monthly precipitation for the area RHA-XII-PY.

2.2.2. Soil-moisture storage capacity

187 Soil-moisture storage capacity STC (equation 3) or water holding capacity (Thornthwaite &
188 Mather, 1955, 1957) is the total amount of water in the soil (reserve) that is susceptible to
189 evapotranspiration (British Columbia & Ministry of Agriculture, 2015). It depends mainly on
190 two factors: the root depth of the vegetation RDV and the available water capacity AWC , which
191 is related to soil characteristics, such as texture, and percentages of organic matter or sands and
192 clays (Thornthwaite & Mather, 1957).

$$193 \quad STC = AWC \cdot RDV \quad (3)$$

194 AWC can also be explained as the water available to plants from the time the soil stops draining
195 water to the time the soil becomes too dry to prevent permanent wilting. It is calculated (equation
196 4) as the difference between field capacity FC and permanent wilting point PWP (British
197 Columbia & Ministry of Agriculture, 2015, Kirkham, 2014, USDA Natural Resources
198 Conservation Service, 1998).

$$199 \quad AWC = FC - PWP \quad (4)$$

² Interpolated climate surfaces for global land areas at a spatial resolution of 30 arc s.

201 FC and PWP can be obtained empirically (equations 5 and 6) considering the
202 percentages of sand (% s) and clay (% c) in the soil, (Saxton & Rawls, 1986) (equations 7 and 8).
203 To obtain the values of AWC for YP, percentages of sand and clay from the soil profiles were
204 taken from INEGI (2014, 2013a).

205
$$FC = \left(\frac{0.3333}{A} \right)^{B^{-1}} \quad (5)$$

206
$$PWP = \left(\frac{15}{A} \right)^{B^{-1}} \quad (6)$$

207 with

208
$$A = \exp(-4.396 - 0.0715(\%c) - 0.000488(\%s)^2 - 0.00004285(\%s)^2(\%c)) \quad (7)$$

210 and

211
$$B = -3.14 - 0.00222(\%c)^2 - 0.00003484(\%s)^2(\%c) \quad (8)$$

212 Land-use / land cover (LULC) plays an important role in the retention of water in the
213 soil. Tropical forests have deeper roots so that water retention is greater than in pastures. The
214 depth of mature roots is given by Thornthwaite and Mather (1957), according to the type of
215 vegetation cover (Table 2). Five categories of typical vegetation-root depths for five different
216 soil types are provided (Charles, 2003). These parameters have been associated with the different
217 land uses given by INEGI (2013b). The 75 different land uses have been grouped according to
218 the maximum root depth ranges (see supplementary information, Table 1). Soil layers and LULC
219 have been integrated with the parameters established for each component so STC values for the
220 entire region can be obtained (Figure 2). The combination of soil and LULC data gives us a
221 specific STC value for each YP area, that ranges from 50 to 300 mm, with an average³ of
222 118 mm, and a standard deviation of 38 mm.

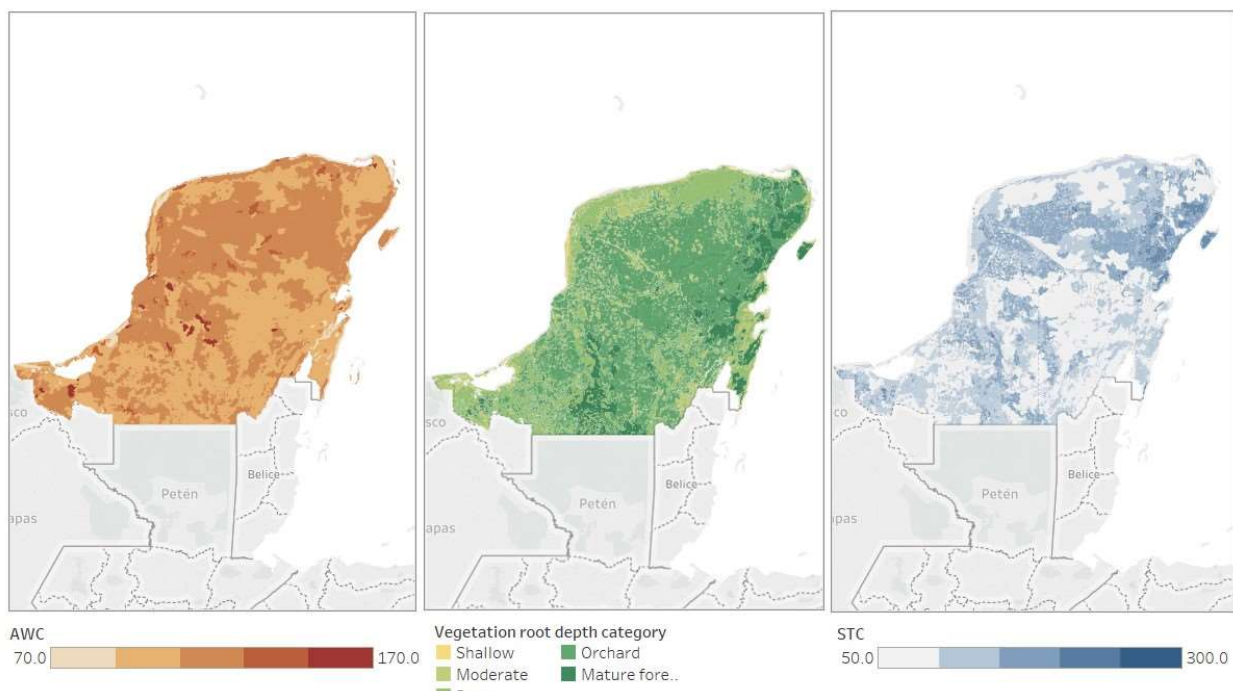
223

³ According Messina and Conner (1998) when STC is unknown, 150 mm is considered as a globally accepted value. For YP $STC = 100$ is a commonly accepted value (Orellana *et al.*, 2009).

224 Table 2. Maximum mature root depth (m). Source: (Charles, 2003, Thornthwaite & Mather,
 225 1957)

Soil Texture Classes	INEGI Classification	Shallow- rooted	Moderately- rooted	Deep-rooted	Orchard	Mature forest
Fine sand	A	0.509	0.762	1.015	1.524	2.539
Fine sandy loams	L	0.509	1.015	1.015	1.692	2.030
Silt loams	Cl	0.634	1.015	1.271	1.524	2.030
Clay loams	Cr	0.405	0.814	1.015	1.015	1.625
Clay	R	0.253	0.509	0.677	0.677	1.189

226



227

228 Figure 2. Left: Soil group (AWC). Center: Vegetation root depth category. Right: Soil-moisture
 229 capacity (STC) in the Yucatan Peninsula

230 2.2.3. Evapotranspiration

231 The estimation of the potential evapotranspiration ET_0 was made with several temperature-
 232 based methods, since temperature is the fundamental and only parameter available in the
 233 definition of the different climate change scenarios (Table 3 and equations 9 to 12). Results are
 234 compared with a ET_0 reference value, estimated globally by FAO (2017).

235 Table 3. List of ET_0 calculation methods considered in this paper.

Method (AKA)	Reference	Formula	Parameters
Thorntwaite (THO)	Thorntwaite (1948)	$ET_o = 16 \left(\frac{10 \times T_i}{I} \right)^\alpha \frac{N}{12} \frac{d}{30}$	[9] T_i, I, α, N, d
Hamon (HAM)	Hamon (1961)	$ET_o = \frac{d \cdot 2.1N^2 \cdot e_s}{T_i + 273.2}$	[10] T_i, e_s, N, d
Hargreaves ⁴ (HAR)	Hargreaves and Samani (1985)	$ET_o = d \cdot 0.0023(T_{max} - T_{min})^{0.424} Ra$	[11] T_{max}, T_{min}, R_a
Blaney-Criddle (BLA)	Blaney and Criddle (1950)	$ET_o = a + bp(0.46T_i + 8.13)$	[12] T_i, a, b, p
Average (AVG)	Combined	<i>Average of all previous</i>	

236

237 The different parameters in Table 3 are defined as follows:

238 • T_i , mean temperature for each month i , in °C.

239 • I , annual heat index, (equation 13):

$$240 I = \sum_{i=1}^{12} \left(\frac{T_i}{5} \right)^{1.514} \quad (13)$$

241 • α , constant (equation 14):

$$242 \alpha = (I^3 \times 675 \times 10^{-9}) - (I^2 \times 771 \times 10^{-7}) + (I \times 1792 \times 10^{-5}) + 0.49239 \quad (14)$$

243 • N , theoretical sunshine hours for each month (equation 15) (R. G. Allen *et al.*, 1998),

$$244 N = \frac{24}{\pi} \omega_s \quad [15]$$

⁴ The exponent of the Hargreaves equation is adjusted from 0.5 to 0.424 according to studies in other regions with similar weather conditions (Tabari *et al.*, 2013).

- ω_s , radiation angle at sunset time, as a function of the latitude (ϕ) and day of the year (R. G. Allen *et al.*, 1998). Here we use the average day of the month, as suggested by Klein (1977).
 - d , number of days for each month.
 - e_s , saturated water vapor density term (equation 16):

$$e_s = 0.6108 \exp\left(\frac{17.27T_i}{T_i + 237.3}\right) \quad (16)$$

- R_a , extraterrestrial radiation for a specific latitude and day (R. G. Allen *et al.*, 1998, Duffie & Beckman, 2013),
 - a and b , model parameters related to wind speed, relative humidity, and current insolation. For YP climate conditions: $a = -1.75$ and $b = 1.06$ (Ponce, 1989),
 - p , percentage of total daytime hours for the period over total daytime hours of the year.

ET_a depends on the precipitation with respect to the potential evapotranspiration, and the available moisture in the soil for each month i (S_i). When P is greater than ET_o , the soil remains humid, and ET_a is equal to ET_o . In this case, S_i is equal to the difference between P_i and $(ET_o)_i$ plus the soil moisture quantity of the previous month (S_{i-1}), as long as the value is less than STC (equations 17 to 19).

$$\text{For } P_i \geq ET_{O_i}, ET_{A_i} = ET_{O_i} \text{ else } ET_{A_i} = P_i + \Delta S_i \quad (17)$$

$$\Delta S_i = S_i - S_{i-1} \quad (18)$$

$$S_i = \min\{(P_i - ET o_i) + S_{i-1}, STC\} \quad (19)$$

264 In contrast, in months when P_i is less than $(ET_o)_i$, the soil dries and $(ET_a)_i$ is lower
 265 than $(ET_o)_i$. Under this circumstance, $(ET_a)_i$ is equal to P_i plus the soil moisture that can be
 266 withdrawn from storage at the end of month i ($\Delta Storage$) (Alley, 1984, Thornthwaite &
 267 Mather, 1955). In this case, S_i is expressed as (equation 20):

$$S_i = S_{i-1} \exp \left[\frac{(P_i - ET_i)}{STC} \right] \quad (20)$$

We can assume that groundwater recharge occurs when P_i exceeds $(ET_o)_i$, and S_i equals STC (equation 21):

$$272 \quad \text{For } P_i \geq ETo_i \text{ and } S_i = STC, \Delta R = (P_i - ETo_i) - (STC - S_{i-1}) \text{ else } 0 \quad (21)$$

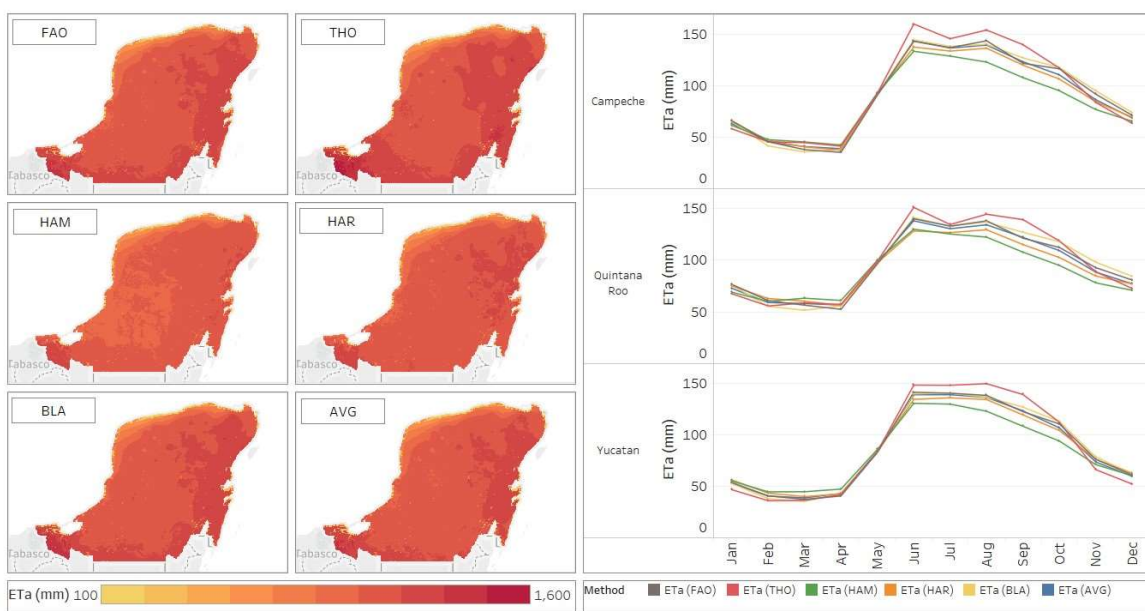
273

274 To initialize the calculation procedure, an assumption is made: S_1 is the last month of the
 275 wet season (September for YP) and is equal to STC (Thorntwaite & Mather, 1957). However,
 276 in regions where annual ET_o is greater than precipitation, available moisture in the soil remains
 277 below STC so a second integration of the procedure is necessary to perform an adjustment to the
 278 initial value of STC , assuming that $S_{13} = S_1$ until reaching $S_{24} = S_{12}$.

According to the 4 methods (Table 3) and FAO's reference ET_o , the average ET_o value for the YP is $1420 \text{ mm} \pm 117 \text{ mm}$, with slight differences between the states:

- Campeche: $1432 \text{ mm} \pm 117 \text{ mm}$
 - Quintana Roo: $1400 \text{ mm} \pm 118 \text{ mm}$
 - Yucatan: $1430 \text{ mm} \pm 118 \text{ mm}$

As shown in figure 3, results⁵ for the different methods show ET_a average values from 1040 mm to 1161 mm. Compared with the rest of the methods, and the FAO reference values, the THO method overestimates ET_a . This is in accordance with observations of Alkaeed et al. (2006), highlighting the inconvenience of using this method for humid climates. Thus, here we do not include this method for obtaining the average value for groundwater recharge.



⁵ Data visualization:

https://public.tableau.com/profile/edgar.rodriguez.huerta#!/vizhome/EstimationActualEvapotranspirationYucatan/ETa_final

289 Figure 3. Left. ET_a in RHA-XII-PY by method. Right ET_a by state and month. (See Table 3 for
290 name method reference)

291

292 **2.3. Climate change scenarios**

293 The effects of climate change in the RHA-XII-PY are based on 4 different General
294 Circulation Models (GCM) and an ensemble average (REA) (Table 4). All GCM contemplate
295 two Representative Concentration Pathways (RCP): 4.5 (low emissions) and 8.5 (high emissions)
296 in the near future 2015-2039. Databases are available in the corresponding climatic atlas update
297 for Mexico (A Fernández Eguiarte *et al.*, 2015a).

298 GCM scenarios of Digital Climatic Atlas of Mexico by Fernandez-Eguiarte A., J. Zavala-
299 Hidalgo. (2010) were developed based on 4 of the 15 models of the project '*Coupled Model*
300 *Intercomparison Project, Phase 5 (CMIP5)*' (Taylor, 2007, Taylor *et al.*, 2012). CMIP5 provides
301 projections of future climate change on two-time scales, near term (out to about 2035) and long
302 term (out to 2100 and beyond). The proposal to establish a period of 25 years (near-future) is
303 based on a new strategy for climate change experiment (Doblas-Reyes *et al.*, 2011, Hibbard *et*
304 *al.*, 2007, Kirtman *et al.*, 2013, Meehl *et al.*, 2009), and is according on the needs of the end
305 users defined in the IPCC workshops (Moss *et al.*, 2007).

306 The adaptation of GCMs to Mexican territory is described in Cavazos *et al.* (2013), and
307 Fernández Eguiarte *et al.* (2015). Downscaling method applied is Change Factor Method (CFM)
308 (Hawkins *et al.*, 2013, Matonse *et al.*, 2011, Navarro-Racines *et al.*, 2015, Tabor & Williams,
309 2010, Wilby *et al.*, 2004). The GCMs were cut in space (0 to 40 N and -140 to -60 W), and the
310 resolution was homogenized ($0.5^\circ \times 0.5^\circ$) by a bilinear interpolation with the CDO platform by
311 Max Planck Institute (Schelzweida, 2019) with the purpose to validate them with several
312 climatological metrics of the East Anglia Climate Research Unit (CRU) (Cavazos *et al.*, 2013).
313 Subsequently, variation layers were obtained by subtracting the GCM (near-future) values with
314 their reference climatology (1961-2000). The new variation grids were subdivided into $30 \times 30''$
315 to preserve the original values of each GCM. Finally, these grids in high resolution were added
316 the corresponding historical monthly values (section 2.2.1) that passed through a process of
317 quality control and that consider the topographic factors.

318

319

320 Table 4. Summary of GCM scenarios

GCM	Institute	Differences RCP 4.5 with historical data		Differences RCP 8.5 with historical data	
		\bar{T} (°C)	P (mm)	\bar{T} (°C)	P (mm)
CNRM-CM5	Centre National de Recherches Meteorologiques	0.67	12.1	0.72	38.4
GFDL_CM3	Geophysical Fluid Dynamics Laboratory	1.31	59.7	1.37	38.9
HADGEM2-ES	Met Office Hadley	1.31	-67.7	1.40	-22.4
MPI_ESM_LR	Max-Plank Institute	0.95	-74.0	1.09	-73.6
Reliability Ensemble Averaging (REA)	weighted assembly projection that considered fifteen GCM	1.37	-57.7	1.43	-58.8
<i>uncertainty of climate projections (\pm)</i>		0.27	52.6	0.27	47.3

322
323 For RCP 4.5, all GCM models estimate an increase in the average annual temperature
324 (\bar{T}), which ranges from 0.67 °C to 1.37 °C, while they reach up to 1.43 °C in RCP 8.5. However,
325 precipitation show a different behavior. Two models estimate an increase in annual precipitation
326 of 12 mm and 60 mm in the estimation of precipitation (CNRM-CM5 and GFDL_CM3), while
327 the other three models estimate a reduction of 66 mm on average (5%).

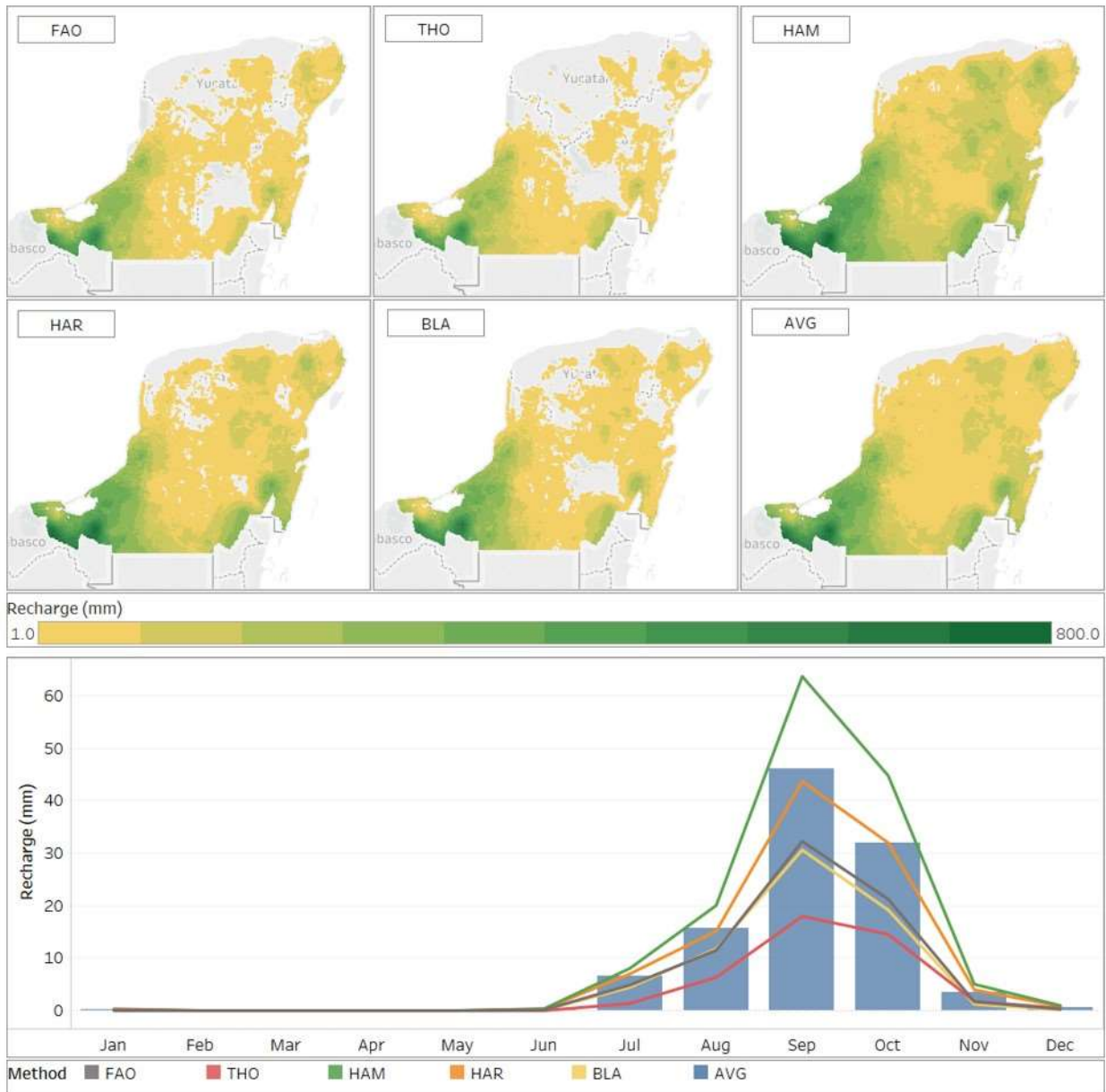
328
329 The different results from this part are obtained in two consecutive steps:

- 330 1. Firstly, a monthly water balance of RHA-XII -PY is performed with the aid of
331 historical climatic data. This is compared with other studies to observe coherence
332 in our results and to validate the model.
- 333 2. Secondly, we apply the same monthly water balance model but this time with
334 estimated climatological data (i.e., precipitation and temperature) for climate
335 change scenarios and for the 2015 -2039 horizon, in order to establish the range of
336 variation in groundwater recharge.

337 **3. Results**

338 ***3.1. Current recharge***

339 According to the different methods, the recharge of RHA-XII-PY varies from 43 mm (THO) to
340 143 mm (HAM), with a recharge around 72 mm if we consider the reference values of FAO
341 (Figure 4). The most important recharge areas are the southwestern and northeastern part of the
342 Campeche and Yucatán states (between Cenotillo and Tizimín municipalities) respectively. In
343 general, the northern coast of Yucatan does not receive a vertical recharge contribution.
344 However, the area receives a contribution by groundwater flow. In addition, Figure 4 shows that
345 the recharge occurs between July and November, being September the month with the highest
346 contribution, with 46 mm average of groundwater recharge in the RHA-XII-PY. The months
347 with the highest groundwater recharge contribution in the model corresponds to the weather-
348 related seasons, being the rainy season for the Yucatan peninsula from June to November, with a
349 peak between August and September (CONAGUA, 2015).



350

351 Figure 4. Recharge of groundwater (mm) simulation. Top: results for ET_a and methods in Table
 352 3. Bottom: monthly recharge for the whole area of the Yucatan Peninsula.

353 **3.2. Sensitivity analysis**

354 Compared to other studies (Table 1), our results tend to underestimate the groundwater recharge.
 355 This can be due to several factors. Firstly, the precipitation data periodicity, since calculations
 356 with monthly data tend to underestimate the groundwater recharge by around 3% compared to
 357 daily data (Rushton & Ward, 1979). Secondly, according to Rushton and Ward (1979),
 358 temperature-based methods underestimate groundwater recharge because they only consider
 359 groundwater recharge when the soil reaches its STC , which constrains the recharge during

360 summer months. This is precisely what happens in our model, which underestimates this value
 361 around 25%. In these particular cases, Lloyd et al. (1966) suggest modifying ET_a calculation for
 362 the months when P is less than ET_o . The reason lies in the evaporation rates of dry soils, which
 363 can be only 10% of the potential evaporation. Finally, it is necessary to analyze the effect of STC
 364 within the model, since usually it is considered as a constant value. To identify these factors, a
 365 sensitivity analysis has been performed considering two scenarios:

- 366 • Variation in ET_a calculation equal to P plus 10% of $ET_o - P$ (equation 22) when P is less
 367 than the ET_o ;

368
$$ET_a = P + 0.1(ET_o - P) \quad (22)$$

- 369 • Null variation in STC , with a constant value of 100 mm for the whole peninsula
 370 (Orellana et al., 2009) to obtain a range closer to the current groundwater recharge (Table
 371 4).

372 Table 5. Groundwater recharge according to model sensitivity analysis factors. A2: Alternative
 373 ET_a (equation 22).

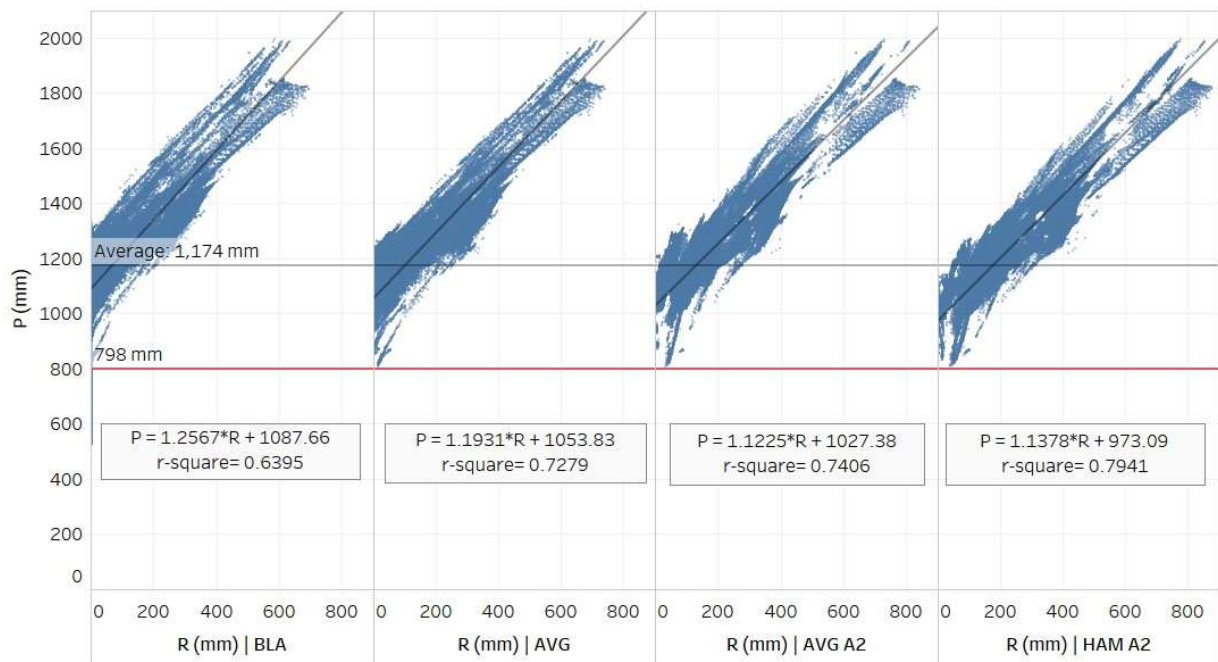
Method	Groundwater recharge (mm)			Percent change (%)	
	Conventional	A2	$STC = 100$	A2	$STC = 100$
FAO	72.5	96.7	80.1	33%	10%
THO	43.3	59.4	45.8	37%	6%
HAM	143.4	176.1	153.1	23%	7%
HAR	102.4	130.0	111.5	27%	9%
BLA	68.2	91.3	74.7	34%	10%
AVG	104.7	132.5	113.1	27%	8%

374
 375 The constant value definition of $STC = 100$, concerning the STC calculated in this study,
 376 represents an increase in the groundwater recharge result of around 8%. This change in the
 377 evaluation of ET_a has an important effect, since it modifies our previous estimation in
 378 approximately 26%, which is aligned with what was reported by Rushton and Ward (1979).
 379 Likewise, we observed that THO method underestimates the groundwater recharge due to the
 380 high values of ET_a , so this method was excluded in the calculation of climate change scenarios.

381 Considering the results shown in table 4, we choose four methods to cover the range of results
 382 obtained by evapotranspiration methods:

- 383 (1) BLA method (Blaney & Criddle, 1950) as the lower limit of the recharge.
- 384 (2) HAM-A2 (Hamon, 1961) with the variation of ET_a calculation described by equation 21
- 385 as the upper limit.
- 386 (3) Averaging results from HAM, BLA, and HAR methods, according to the methodology
- 387 of Alley (1984), to obtain ET_a (equation 17 –20) (AVG).
- 388 (4) Considering the calculation of ET_a according to Lloyd et al. (1966) (equation 22).
- 389 Numbers 3 and 4 as intermediate values (AVG-A2).

390 As expected, there is a direct correlation between precipitation and recharge (Figure 5).
 391 We integrate the recharge results with the RHA-XII-PY precipitation data, in order to generate a
 392 scatterplot and to identify the relationship that exists between them. In addition to the linear
 393 correlation between recharge and precipitation (which serves to make a simple estimate of the
 394 recharge from precipitation), a limiting value is observed, where no recharge is produced below
 395 798 mm annual rainfall (Figure 5, red horizontal line). This is a remarkable outcome since it
 396 suggests that a region with annual rainfall below this threshold, will stop receiving natural
 397 recharge by infiltration.



398
 399 Figure 5. Correlation between precipitation P and recharge R for every grid (926 x 926 m
 400 approximately).

402 **3.3. Climate change effects**

403

404 When we include ET_o and ET_a values from previous models into the different climate change
 405 projections, results show an average annual recharge of $91 \text{ mm} \pm 39 \text{ mm}$, and $94 \text{ mm} \pm 38 \text{ mm}$,
 406 for RCP 4.5 and RCP 8.5 respectively. This represents a 22% reduction in groundwater recharge,
 407 based on historical data. Table 6 shows recharge values for each method according to the
 408 precipitation and temperature estimations of the climate change projections. We observe that an
 409 increase in the representative concentration pathway from 4.5 to 8.5, implies a slight reduction in
 410 recharge: between 1% and 2%. Results on the percentage of change with respect to current
 411 recharge values depend on the chosen methodology: methods that only use mean temperatures
 412 for the calculation of ET_o (i.e., HAM and BLA) give the highest recharge decrease (around
 413 24%); the method that includes maximum and minimum temperatures (i.e., HAR) gives a
 414 decrease of approximately 13%.

415 Table 6. Effects of climate change on groundwater recharge in YP. Projections shown for RCP
 416 4.5 and 8.5 include error and percentage change with respect to current values.

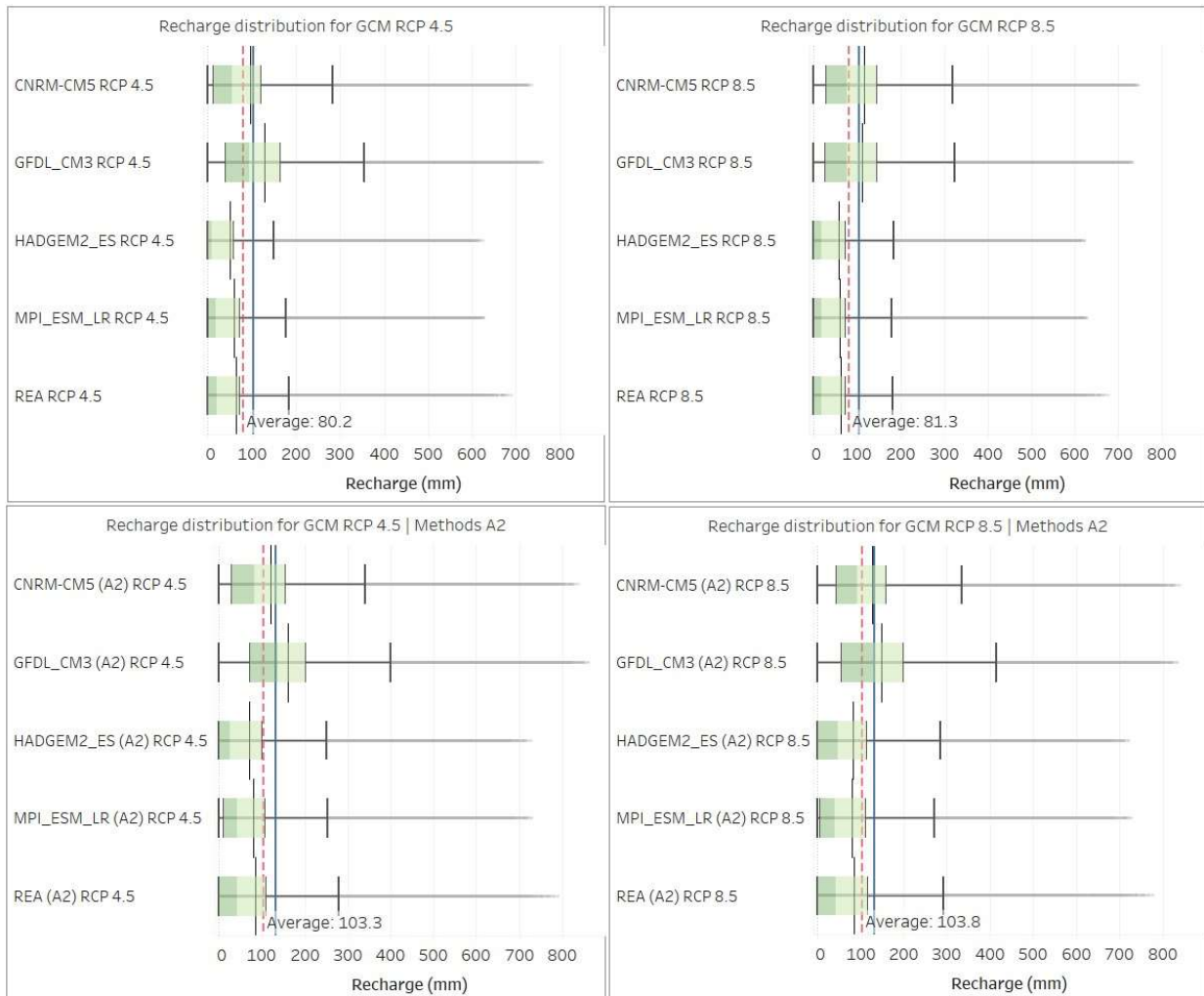
417

ET_a calculation	Method	Current	Recharge (mm)		Percentage change (%)	
			RCP 4.5	RCP 8.5	RCP 4.5	RCP 8.5
Conventional	HAM	143.4	101.8 \pm 39.4	103.5 \pm 35.7	-29%	-28%
	HAR	102.4	87.8 \pm 34.7	90.3 \pm 30.4	-14%	-12%
	BLA	68.2	53.3 \pm 24.2	53.7 \pm 21.0	-22%	-21%
	AVG	104.7	77.5 \pm 32.6	79.0 \pm 28.9	-26%	-25%
A2	HAM	176.1	130.4 \pm 42.8	134.7 \pm 40.6	-26%	-24%
	HAR	130.0	111.5 \pm 40.3	116.6 \pm 37.1	-14%	-10%
	BLA	91.3	70.1 \pm 30.3	72.6 \pm 27.9	-23%	-20%
	AVG	132.5	100.9 \pm 38.3	104.6 \pm 35.5	-24%	-21%

418

419 Four out of five climate change projections (Figure 6) have negative effects on
 420 groundwater recharge, being HADGEM2_ES the most dramatic one, with average ranging from
 421 51 mm to CNRM CM5 (A2) with 120 mm. Model GFDL_CM3 estimates an increase in
 422 recharge, from 129 mm to 161 mm with RCP 4.5 (approximately 22% of the recharge with
 423 historical data) and from 112 to 147 mm with RCP 8.5 (an increase of 10%). Only in the case of

424 RCP 8.5 with A2 methods for ET_a estimation, GFDL_CM and CNRM-CM5 give higher values
 425 than the recharge ones with historical data.



426
 427 Figure 6. Recharge distribution for GCM RCP 4.5 and RCP 8.5. Blue continuous line: Average
 428 recharge with historical data. Red dashed line: GCM average.
 429

430 The effect on groundwater recharge across the Yucatan peninsula is certainly heterogeneous. Our
 431 models give different patterns of recharge distribution as a result of the effects of climate change
 432 on each state of the peninsula. According to our results, the recharge will certainly decrease, with
 433 the most relevant effects in the center and northwest, presenting a high risk of not receiving
 434 vertical recharge in these areas.

435 4. Discussion and conclusions

436 Given the irregular and thin thickness of soil layer of the YP, the infiltration from meteoric

437 recharge (precipitation) is fast, due to fractures, and it's drained to the aquifer. This supports the
438 idea that base flow comes from the interior of the Peninsula (Neuman & Rahbek, 2007).
439 Groundwater recharge levels around $118 \pm 33 \text{ mm} \cdot \text{year}^{-1}$ obtained by our model are in
440 agreement with the estimation obtained with a simple water-balance calculation by Lesser (1976)
441 of $150 \text{ mm} \cdot \text{year}^{-1}$ (around 14% of mean annual precipitation), and by Back (1985), Hanshaw &
442 Back (1980), with similar results of Lesser (1976). However, Beddows (2004) estimated a
443 groundwater recharge between 30 and 70% of mean precipitation for Quintana Roo coast.
444 Recently, Gondwe et al. (2010) computed a recharge value equivalent to 17% of average
445 precipitation.

446 We consider different methods for ET_O estimation, that allow us to assess uncertainties in
447 this variable in this particular case study. Our model presents a conservative estimate, since it is
448 based on a monthly water balance, and, as mentioned in section 2.2, it dismisses the submarine
449 groundwater discharge (SGD), as well as some parameters of hydraulic diffusivity and
450 transmissivity that determine the groundwater flow and storage through the porosity and
451 fractures of the karstic aquifer (Bakalowicz, 2005). At the same time, it also dismisses
452 groundwater flows, caused mainly by karstic aquifer (González-Herrera et al., 2002, Perry et al.,
453 2009). These flows are assumed to run radially across YP, following the belt of sinkholes
454 (cenotes) (González-Herrera et al., 2002, Steinich & Marín, 1997), starting from Sierrita de
455 Ticul (main physiographic feature with a maximum elevation of 275 meters above sea level)
456 located in the southern of YP, about 70 km south of Mérida (Marín-Stillman et al., 2008) and
457 ending at the northern coast of the peninsula.

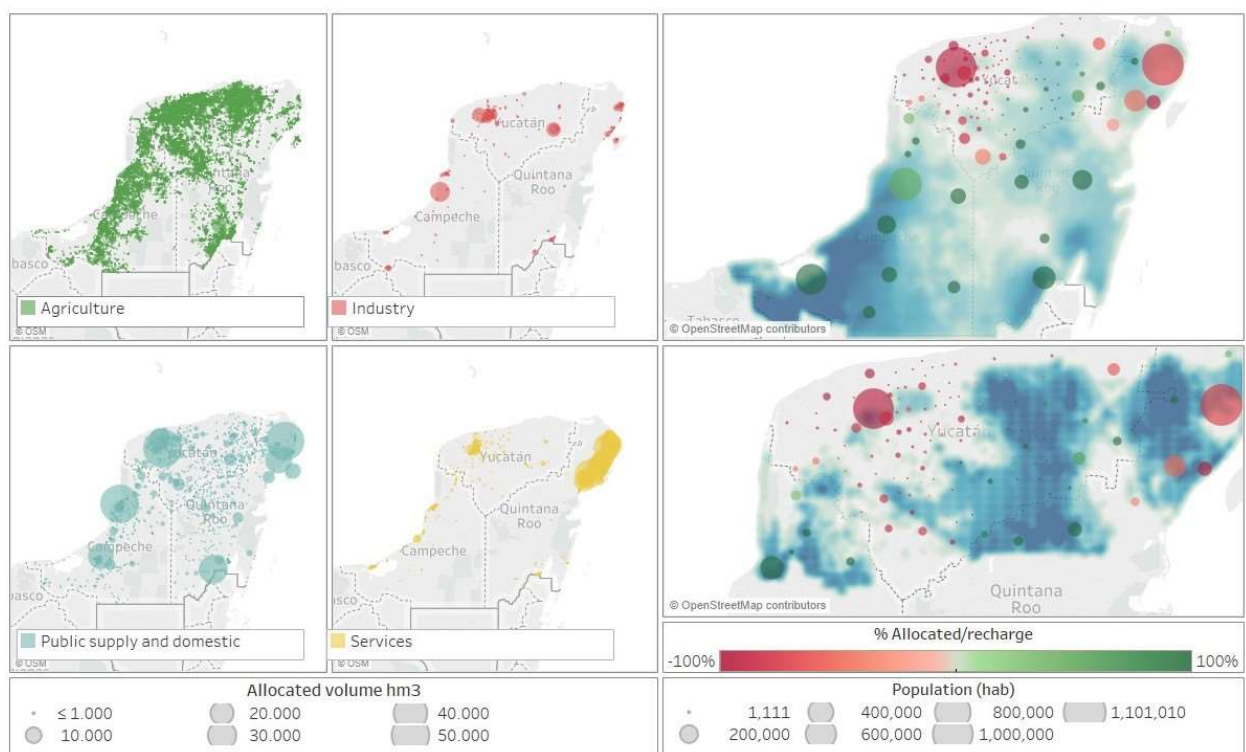
458 According to Bauer-Gottwein et al. (2011), further research is needed in order to estimate
459 precisely the groundwater recharge magnitudes for the YP karst aquifer and coastal outflow from
460 the aquifer to the ocean.

461 **4.1. Recharge and water use**

462
463 When we disaggregate our results at the state-municipality level, we can compare
464 allocated volume for different uses (CONAGUA, 2017) with groundwater recharge for each
465 municipality. Although basic (because it does not consider underground flows to the coast), this
466 process allows the generation of an 'elementary local water ecological footprint' to determine if it
467 is possible to satisfy the regional needs by only covering its 'theoretical' recharge within the
468 administrative boundaries, and only exploiting the aquifer flows that go from south to north,
469 without affecting or intervening in the recharge of neighboring municipalities. We identify sub-

470 regions where recharge modifications will be most critical in Figure 7, considering method
 471 AVG-A2 with GCM CNRM-CM5 RPC 4.5. Location of water permits in YP for every
 472 economic sector are shown in Figure 7 (left), with the extension of agricultural activities,
 473 industrial hubs, and main urban and tourism (i.e., services) areas on the Caribbean coast.
 474 Municipalities (in population size) and vertical recharge distribution of the groundwater (with
 475 GCM results considered as background) are shown in Figure 7 (right), where color indicates the
 476 ratio between allocated (i.e., use) and recharge water values.

477 Municipalities at the northwest region (: i.e., North-Yucatan (32) hydrological basin)
 478 present the worst ratio (i.e., ~ - 66%). With a population of ~ 2,000,000 (45% of the YP
 479 population), this region has an actual water consumption of 935 hm³ (72% primary sector, 4%
 480 secondary, 2% tertiary, 22% public supply), which represents 20% of the water use in YP
 481 (CONAGUA, 2017). However, due to the demographic growth of 20% expected by 2030
 482 (CONAPO, 2010), with an industrial growth in the area linked to the hub port in Progreso,
 483 associated with the tourism potential of the coastal zone, water consumption and demand will
 484 possibly increase at a higher rate in the upcoming years.



485
 486 Figure 7. Left: Water uses in YP by sector, size allocated volume (hm³). Right:
 487 recharge and uses by municipality as color. Population as size.

488 Official data (CONAGUA, 2019) refer to recharge (and renewable water) as an average
 489 result across the YP. Studies on the estimation of recharge on a smaller scale raise awareness

490 about the differences that exist within the same territory. The application of downscaling
491 methods in climatological data, and in climate change scenarios like the method developed by
492 Fernández Eguiarte *et al.* (2015) provides more precise information at geographical level than
493 the average recharge of groundwater, habitually used, and even questionable from a regional
494 point of view. Water balance at a lower scale improves our ability to understand and estimates
495 the effects of climate change on water availability.

496 Regionalization contributes to information support, planning of productive activities,
497 defining the growth of specific areas where the resource may be compromised; and should be
498 considered before allocating water uses, in such a way, avoided locating large extractions in sub-
499 regions with potential risk or vulnerability. For example, the last major water allocation in
500 Yucatan –with 7 hm³ per year, around 26% of water for industrial use (excluding electricity-
501 generation)– (CONAGUA, 2017, Consultores en Prevención y Mitigación de Impactos
502 Ambientales, 2015), was assigned after the environmental impact statement justified the
503 application of projects in Yucatan, because the region (the whole peninsula) has a high annual
504 availability of groundwater, and therefore, ‘*will not cause the affectation, stress or significant
505 decrease of the water of the subsoil*’.⁶ However, the project is located in areas where vertical
506 recharge, as well as availability, is much lower than the average of the entire hydrological region
507 (Figure 7) and does not consider specifications about the actual availability and the effects of the
508 urban contexts that are located to the north, and that will reduce their groundwater flow for their
509 supply.

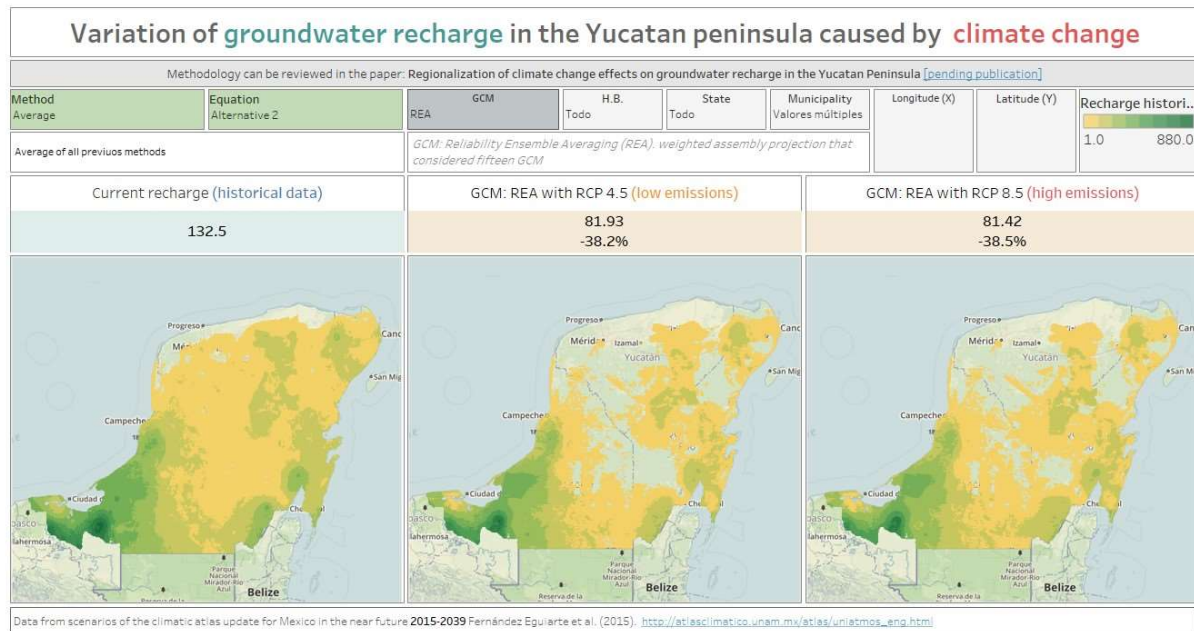
510 In this sense, vertical recharge of groundwater (from precipitation) is only one
511 component within a more complex system such as the water cycle, and further research needs to
512 be conducted to analyze the effects on water demand at different spatial level, as well as the
513 groundwater flows in the region, which could buffer the effects of climate change in northern
514 region of YP.

515 Our study serves as a new reference to describe the problemshed of groundwater in
516 Yucatan Peninsula. It is a starting point to assess the region's renewable water (mostly from
517 groundwater) considering future demand and socio-economic characteristics.

518 With the objective of exploring climate change effects on groundwater recharge in the
519 Yucatan Peninsula at different spatial levels our results, open and freely available, have been

⁶ Chapter III. Section: conservation criteria, point 12 (Consultores en Prevención y Mitigación de Impactos Ambientales, 2015)

520 transferred to a dashboard⁷ to compare specific regions (from map cell (926 m x 926 m),
 521 municipality, state or hydrological basin (Figure 8). This data visualization tool expects to be and
 522 auxiliary display for decision making support, with the objective to simplify the analysis and to
 523 deepen into the geographic and socioecological dimensions of water in the Yucatán Peninsula.



524
 525 Figure 8. Variation of groundwater recharge in the Yucatan peninsula caused by climate change.
 526 Dashboard in Tableau ® (Rodríguez-Huerta, 2018)
 527

528 ***4.2. Interaction of groundwater and vegetation***

529 Furthermore, water balance, vegetation and soil dynamics are complex with multiple
 530 feedback loops (Asbjornsen *et al.*, 2011, Rodríguez-Iturbe, 2000). Several models (Breshears &
 531 Barnes, 1999, Huisman *et al.*, 2009, Kefi *et al.*, 2008, Li *et al.*, 2009, Shnerb *et al.*, 2003, Zhou *et*
 532 *al.*, 2015) describe how alterations in the hydrological cycle change vegetation patterns. A
 533 decrease in precipitation will cause greater competition over this resource, which will initiate
 534 adjustments in the vegetation. In the first instance, reducing the density of the cover, generating
 535 vegetation patterns, and converting what was a uniform cover into another with areas of bare soil
 536 until reaching a new equilibrium of the ecosystem (Kefi *et al.*, 2008, Klausmeier, 1999, Shnerb

⁷ <https://public.tableau.com/profile/edgar.rodriguez.huerta#!/vizhome/GroundwaterrechargeYucatanPeninsula/VIZ>

537 *et al.*, 2003, Solé, 2011). These interactions can be studied from the theory of complex systems
538 and open a future line of research of the effects of climatic change in YP.

539 **5. Acknowledgments**

540 This work was supported by CONACYT-Mexico under PhD grant number 220474.

541 **6. References**

- 542 Alan, E., José, E., Romero, A., Irving, M. & Hernández Gómez, U. (2015) *Evaluación y mapeo*
543 *de los determinantes de la deforestación en la Península Yucatán*. México, Distrito Federal:
544 Agencia de los Estados Unidos para el Desarrollo Internacional (USAID), The Nature
545 Conservancy (TNC), Alianza México REDD+. Retrieved from http://www.alianza-mredd.org/uploads/ckfinder_files/files/1_INFORME DETERMINANTE DEFORESTACION PY .pdf
- 546 Albornoz-Euán, Beth I. (2007) *Análisis de riesgo de contaminación de aguas subterráneas*
547 *utilizando sistemas de información geográfica*. Universidad Autónoma de Yucatán.
- 548 Albornoz-Euán, Bethsua Iztaccihuatl, González-Herrera, R. A., Albornoz-Euán, B. S. I. &
549 González-Herrera, R. A. (2017) Vulnerabilidad a la contaminación del acuífero yucateco
550 bajo escenarios de cambio climático. *Ecosistemas y Recur. Agropecu.* **4**(11), 275.
551 Universidad Juárez Autónoma de Tabasco, Dirección de Investigación y Posgrado.
552 doi:10.19136/era.a4n11.1037
- 553 Ali, R., McFarlane, D., Varma, S., Dawes, W., Emelyanova, I., Hodgson, G. & Charles, S.
554 (2012) Potential climate change impacts on groundwater resources of south-western
555 Australiarn Australia. *J. Hydrol.* **475**, 456–472. Elsevier B.V.
556 doi:10.1016/j.jhydrol.2012.04.043
- 557 Alkaeed, O., Flores, C., Jinno, K. & Tsutsumi, A. (2006) Comparison of several reference
558 evapotranspiration methods for Itoshima Peninsula Area, Fukuoka, Japan. *Mem. Fac. Eng.
Kyushu Univ.* **66**(1), 1–14. doi:Vol. 66, No.1, March 2006
- 559 Allen, D. M., Cannon, A. J., Toews, M. W. & Scibek, J. (2010) Variability in simulated recharge
560 using different GCMs. *Water Resour. Res.* **46**(10), 1–18. doi:10.1029/2009WR008932
- 561 Allen, R. G., Pereira, L. S., Raes, D. & Smith, M. (1998) Crop evapotranspiration: Guidelines for
562 computing crop requirements. *Irrig. Drain. Pap. No. 56, FAO* (56), 300.
563 doi:10.1016/j.eja.2010.12.001

- 567 Alley, W. M. (1984) On the Treatment of Evapotranspiration, Soil Moisture Accounting, and
568 Aquifer Recharge in Monthly Water Balance Models. *Water Resour. Res.* **20**(8), 1137–
569 1149. doi:10.1029/WR020i008p01137
- 570 Aranda-Cirerol, N., Comín, F. & Herrera-Silveira, J. (2010) Nitrogen and phosphorus budgets
571 for the Yucatán littoral: An approach for groundwater management. *Environ. Monit. Assess.*
572 **172**(1–4), 493–505. doi:10.1007/s10661-010-1349-z
- 573 Asbjornsen, H., Goldsmith, G. R., Alvarado-Barrientos, M. S., Rebel, K., Osch, F. P. Van,
574 Rietkerk, M., Chen, J., et al. (2011) Ecohydrological advances and applications in plant-
575 water relations research: A review. *J. Plant Ecol.* **4**(1–2), 3–22. doi:10.1093/jpe/rtr005
- 576 Back, W. (1985) Hydrogeology of the Yucatan. In: *Geology and hydrogeology of the Yucatan*
577 and quaternary geology of northeastern Yucatan Peninsula, 99–124. New Orleans : LA:
578 Published by New Orleans Geological Society,. Retrieved from
579 <https://searchworks.stanford.edu/view/1606188>
- 580 Bakalowicz, M. (2005) Karst groundwater: A challenge for new resources. *Hydrogeol. J.* **13**(1),
581 148–160. doi:10.1007/s10040-004-0402-9
- 582 Bates, B. C., Kundzewicz, Z. W., Wu, S. & Palutikof, J. P. (2008) *Climate Change and Water:*
583 *Technical Paper of the Intergovernmental Panel on Climate Change.* (IPCC Secretariat,
584 Ed.), 2008th ed. Geneva. Retrieved from
585 <http://41.73.194.134:8080/xmlui/bitstream/handle/123456789/552/climate-change-water->
586 [en.pdf?sequence=1](#)
- 587 Bauer-Gottwein, P., Gondwe, B. R. N., Charvet, G., Marín, L. E., Rebollo-Vieyra, M. &
588 Merediz-Alonso, G. (2011) Review: The Yucatán Peninsula karst aquifer, Mexico.
589 *Hydrogeol. J.* **19**(3), 507–524. doi:10.1007/s10040-010-0699-5
- 590 Beddows, P. A. (2004) *Groundwater hydrology of a coastal conduit carbonate aquifer:*
591 *Caribbean coast of the Yucatán Peninsula, México, PhD Thesis.* University of Bristol, UK.
592 Retrieved from <http://ethos.bl.uk/OrderDetails.do?uin=uk.bl.ethos.398776>
- 593 Blaney, H. F. & Criddle, W. (1950) Determining water requirements in irrigated areas from
594 climatological and irrigation data. *Tech. Pap. U.S. Soil Conserv. Serv.* No. **96**(Washington,
595 D.C.), 48 pp. Retrieved from <http://agris.fao.org/agris-search/search.do?recordID=US201300593774>
- 597 Breshears, D. D. & Barnes, F. J. (1999) Interrelationships between plant functional types and soil

- 598 moisture heterogeneity for semiarid landscapes within the grassland/forest continuum: a
599 unified concept. *Landsc. Ecol.* **14**(5), 465–478. doi:10.1023/A:1008040327508
- 600 British Columbia & Ministry of Agriculture. (2015) Soil water storage capacity and available
601 soil moisture. *Water Conserv. Factsheet 619.000–1*. Retrieved from
602 https://www2.gov.bc.ca/assets/gov/farming-natural-resources-and-industry/agriculture-and-seafood/agricultural-land-and-environment/soil-nutrients/600-series/619000-1_soil_water_storage_capacity.pdf
- 603
- 604
- 605 Carballo Parra, R. M. (2016) *Identificación del flujo subterráneo como consecuencia de la*
606 *incidencia de plaguicidas y de cargas hidráulicas en una zona de campo de golf de la*
607 *Riviera Maya*. Centro de Investigaciones Científica de Yucatán, A.C. Retrieved from
608 https://cicy.repositorioinstitucional.mx/jspui/bitstream/1003/367/1/PCA_M_Tesis_2016_Carballo_Rocio.pdf
- 609
- 610 Cervantes Martínez, A. (2007) El balance hídrico en cuerpos de agua cársticos de la Península de
611 Yucatan. *Teoría y Prax.* **3**, 143–152.
- 612 Charles, E. (2003) A Method for Evaluating Ground-Water-Recharge Areas in New Jersey. *New*
613 *Jersey Geol.* Retrieved from <http://www.nj.gov/dep/njgs/pricelst/gsreport/gsr32.pdf>
- 614 CONAGUA. (2015) Estadísticas del agua en México. Edición 2015 (1), 1–5.
615 doi:10.1007/s13398-014-0173-7.2
- 616 CONAGUA. (2015) Actualización de la disponibilidad media anual de agua en el acuífero
617 Península de Yucatán (3105), Estado de Yucatán. doi:10.1017/CBO9781107415324.004
- 618 CONAGUA. (2016) Atlas del agua en México 2015. México. Retrieved from
619 www.conagua.gob.mx
- 620 CONAGUA. (2017) SINA 2.0. Retrieved April 27, 2017, from
621 http://sina.conagua.gob.mx/sina/index_jquery-mobile2.html?tema=usosAqua
- 622 CONAGUA. (2019) Estadísticas de Agua en México. 2018. Ciudad de México, México.
623 Retrieved from http://sina.conagua.gob.mx/publicaciones/EAM_2018.pdf
- 624 CONAGUA & SEMARNAT. (2012) Programa Hídrico Regional Visión 2030. MEXICO.
625 Retrieved from <http://www.conagua.gob.mx/conagua07/publicaciones/publicaciones/12-sgp-17-12py.pdf>
- 626
- 627 CONAPO. (2010) Dinámica demográfica 1990-2010 y proyecciones de población 2010-2030

- 628 Yucatán. Retrieved from
629 http://www.conapo.gob.mx/work/models/CONAPO/Proyecciones/Cuadernos/31_Cuadernil
630 lo_Yucatan.pdf
- 631 Consultores en Prevención y Mitigación de Impactos Ambientales. (2015) Manifiesto de impacto
632 ambiental para la construcción y operación de infraestructura de Servicios en Cervecería
633 Yucateca. Mérida.
- 634 Dale, V. H., Joyce, L. a, McNulty, S., Neilson, R. P., Ayres, M. P., Flannigan, M. D., Hanson, P.
635 J., et al. (2001) Climate Change and Forest Disturbances **51**(9), 723–734.
- 636 Doblas-Reyes, F. J., Oldenborgh, G. J. van, García-Serrano, J., Pohlmann, H., Scaife, A. A. &
637 Smith, D. (2011) CMIP5 near-term climate prediction. *CLIVAR Exch.* **16**(2), 8–11.
- 638 Dore, M. H. I. (2005) Climate change and changes in global precipitation patterns: What do we
639 know? *Environ. Int.* **31**(8), 1167–1181. Pergamon. doi:10.1016/J.ENVINT.2005.03.004
- 640 Duffie, J. A. & Beckman, W. A. (2013) *Solar engineering of the thermal processes*, 4th ed.
641 Wiley. Retrieved from <https://www.advan-kt.com/solarengineering.pdf>
- 642 Estrada Medina, H. & Cobos Gasca, V. (2012) Programa Nacional contra la sequía
643 PRONACOSE. Mérida.
- 644 FAO. (2017) Global map of monthly reference evapotranspiration - 5 arc minutes. Retrieved
645 March 6, 2018, from <http://ref.data.fao.org/map?entryId=db326f70-88fd-11da-a88f-000d939bc5d8>
- 647 Fernandez-Eguiarte A., J. Zavala-Hidalgo., R. R.-C. (2010) Digital climatic Atlas of Mexico.
648 *Cent. Ciencias la Atmósfera, UNAM*. Retrieved from
649 http://atlasclimatico.unam.mx/atlas/uniatmos_eng.html
- 650 Fernández Eguiarte, A, Zavala Hidalgo, J., Romero Centeno, R., Conde Álvarez, A. & Trejo
651 Vázquez, R. (2015) Actualizacion de los escenarios de cambio climatico para estudios de
652 impactos, vulnerabilidad y adaptacion. *Climatol. Ref. SMN 1961 - 2000*. Retrieved
653 November 7, 2018, from http://atlasclimatico.unam.mx/AECC_descargas/
- 654 Fernández Eguiarte, A, Zavala Hidalgo, J., Romero Centeno, R., Conde Álvarez, A. & Trejo
655 Vázquez, R. (2015) Actualización de los escenarios de cambio climático para estudios de
656 impactos, vulnerabilidad y adaptación. Centro de Ciencias de la Atmósfera, Universidad
657 Nacional Autónoma de México. Instituto Nacional de Ecología y Cambio Climático,
658 Secretaría de Medio Ambiente y Recursos Naturales. doi:04-2011-120915512800-203

- 659 Fernández Eguiarte, Agustín, Romero Centeno, R. & Zavala Hidalgo, J. (2014) Methodologies
660 used in the digital climatic atlas of Mexico for generating high-resolution maps. *GEOACTA*
661 **39**(1), 165–173. Retrieved from <http://www.scielo.org.ar/pdf/geoacta/v39n1/v39n1a13.pdf>
- 662 Findlay, R. (2003) Global climate change: implications for water quality and quantity. *Am.*
663 *Water Work. Assoc.* **95**(9), 36.
- 664 Gao, L., Huang, J., Chen, X., Chen, Y. & Liu, M. (2018) Contributions of natural climate
665 changes and human activities to the trend of extreme precipitation.
666 doi:10.1016/j.atmosres.2018.02.006
- 667 Gondwe, B. R. N., Lerer, S., Stisen, S., Marín, L. & Rebollo-Vieyra, M. (2010) Hydrogeology
668 of the south-eastern Yucatan Peninsula: New insights from water level measurements,
669 geochemistry, geophysics and remote sensing. *J. Hydrol.* **389**(1–2), 1–17. Elsevier.
670 doi:10.1016/J.JHYDROL.2010.04.044
- 671 González-Herrera, R., Sánchez-y-Pinto, I. & Gamboa-Vargas, J. (2002) Groundwater-flow
672 modeling in the Yucatan karstic aquifer, Mexico. *Hydrogeol. J.* **10**(5), 539–552.
673 doi:10.1007/s10040-002-0216-6
- 674 Green, T. R., Taniguchi, M., Kooi, H., Gurdak, J. J., Allen, D. M., Hiscock, K. M., Treidel, H., et
675 al. (2011) Beneath the surface of global change: Impacts of climate change on groundwater.
676 *J. Hydrol.* **405**(3–4), 532–560. Elsevier B.V. doi:10.1016/j.jhydrol.2011.05.002
- 677 Grobick, A. (2010) Managing water for green growth: Supporting climate adaptation and
678 building climate resilience. *Sustain. Water* 118–121. Retrieved from
679 http://www.gwp.org/Global/Events/COP16/Managing Water for Green Growth_Dr_Grobicki article.pdf
- 681 Hamon, W. R. (1961) Estimating potential evapotranspiration. *J. Hydraul. Div.*
- 682 Hanshaw, B. B. & Back, W. (1980) Chemical mass-wasting of the northern Yucatan Peninsula
683 by groundwater dissolution. *Geology* **8**(5), 222. GeoScienceWorld. doi:10.1130/0091-7613
684 (1980)
- 685 Herrera-Pantoja, M. & Hiscock, K. M. (2008) The effects of climate change on potential
686 groundwater recharge in Great Britain. *Hydrol. Process.* **22**, 73–86. doi:10.1002/hyp.6620
- 687 Hibbard, K. A., Meehl, G. A., Cox, P. M. & Friedlingstein, P. (2007) A strategy for climate
688 change stabilization experiments. *Eos (Washington. DC)*. **88**(20), 217–221.
689 doi:10.1029/2007EO200002

- 690 Hijmans, R. J., Cameron, S. E., Parra, J. L., Jones, P. G. & Jarvis, A. (2005) Very high resolution
691 interpolated climate surfaces for global land areas. *Int. J. Climatol.* **25**(15), 1965–1978.
692 doi:10.1002/joc.1276
- 693 Holliday, L., Marin, L. & Vaux, H. (2007) *Sustainable management of groundwater in Mexico. Strength. Sci. Decis. Sustain. Manag. Gr. Water Mex. Work. Proc. held.* Washington, DC:
694 National Academy of Sciences. Retrieved from
695 <http://www.nap.edu/catalog/11875.html%0AVisit>
- 696 Holman, I. P., Allen, D. M., Cuthbert, M. O. & Goderniaux, P. (2012) Towards best practice for
697 assessing the impacts of climate change on groundwater. *Hydrogeol. J.* **20**(1), 1–4.
698 doi:10.1007/s10040-011-0805-3
- 700 Huebener, H., Cubasch, U., Langematz, U., Spangehl, T., Niehörster, F., Fast, I. & Kunze, M.
701 (2007) Ensemble climate simulations using a fully coupled ocean-troposphere-stratosphere
702 general circulation model. *Philos. Trans. A. Math. Phys. Eng. Sci.* **365**(1857), 2089–101.
703 The Royal Society. doi:10.1098/rsta.2007.2078
- 704 Huisman, J. A., Breuer, L., Bormann, H., Bronstert, A., Croke, B. F. W., Frede, H. G., Gräff, T.,
705 et al. (2009) Assessing the impact of land use change on hydrology by ensemble modeling
706 (LUCHEM) III: Scenario analysis. *Adv. Water Resour.* **32**(2), 159–170. Elsevier Ltd.
707 doi:10.1016/j.advwatres.2008.06.009
- 708 INEGI. (2002) Estudio hidrológico del estado de Yucatán.
709 doi:10.1017/CBO9781107415324.004
- 710 INEGI. (2013) Conjunto de datos de Perfiles de suelos. Escala 1:250 000. Serie II (Continuo
711 Nacional). Retrieved March 10, 2018, from
712 <http://www.beta.inegi.org.mx/app/biblioteca/ficha.html?upc=702825266707>
- 713 INEGI. (2013) Uso de suelo y vegetación, escala 1:250000, serie V. Retrieved November 2,
714 2016, from <http://www.conabio.gob.mx/informacion/gis/>
- 715 INEGI. (2014) Diccionario de datos edafológicos. Escala 1:250,000 (versión 3). México.
716 Retrieved from
717 http://www.inegi.org.mx/geo/contenidos/recnat/edafologia/doc/dd_edafologicos_v3_250k.pdf
- 718 df
- 719 INEGI. (2015) Anuario estadístico y geográfico de Yucatán. México. Retrieved from
720 http://internet.contenidos.inegi.org.mx/contenidos/productos//prod_serv/contenidos/espanol

- 721 /bvinegi/productos/nueva_estruc/anuarios_2015/702825077235.pdf
- 722 IPCC. (2007) *Climate Change 2007 The Physical Science Basis The. Contrib. Work. Gr. I to*
723 *Fourth Assess. Rep. IPCC*, Vol. 53. doi:10.1017/CBO9781107415324.004
- 724 IPCC. (2013) What is a GCM? Retrieved April 30, 2018, from http://www.ipcc-data.org/guidelines/pages/gcm_guide.html
- 725 Jauregui, E. (2005) Impact of Increasing Urbanization on the Thermal Climate of Large Mexican
726 Cities. *Fifth Int. Conf. Urban Clim.* **18**(4), 247–248. Retrieved from
727 http://www.geo.uni.lodz.pl/~icuc5/text/O_22_3.pdf
- 728 Kefi, S., Rietkerk, M. & Katul, G. G. (2008) Vegetation pattern shift as a result of rising
729 atmospheric CO₂ in arid ecosystems. *Theor. Popul. Biol.* **74**(4), 332–344. Elsevier Inc.
730 doi:10.1016/j.tpb.2008.09.004
- 731 Kirkham, M. B. (2014) Field Capacity, Wilting Point, Available Water, and the Nonlimiting
732 Water Range. In: *Principles of Soil and Plant Water Relations*, 153–170.
733 doi:10.1016/B978-0-12-420022-7.00010-0
- 734 Kirtman, B., Power, S. B., Adedoyin, J. A., Boer, G. J., Bojariu, R., Camilloni, I., Doblas-Reyes,
735 F. J., et al. (2013) Near-term Climate Change Projections and Predictability. In: *Climate
736 Change 2013: The Physical Science Basis. Contribution of Working Group I to the Fifth
737 Assessment Report of the Intergovernmental Panel on Climate Change* (V. B. and P. M. M.
738 (eds.)]. [Stocker, T.F., D. Qin, G.-K. Plattner, M. Tignor, S.K. Allen, J. Boschung, A.
739 Nauels, Y. Xia, ed.), 982–985. Cambridge, United Kingdom and New York, NY, USA.:
740 Cambridge University Press. doi:10.1017/CBO9781107415324.023
- 741 Klausmeier, C. A. (1999) Regular and irregular patterns in semiarid vegetation. *Science* (80-.).
742 **284**(5421), 1826–1828. doi:10.1126/science.284.5421.1826
- 743 Klein, S. A. (1977) Calculation of monthly average insolation on tilted surfaces. *Sol. Energy*
744 **19**(4), 325–329. Pergamon. doi:10.1016/0038-092X(77)90001-9
- 745 Kløve, B., Ala-Aho, P., Bertrand, G., Gurdak, J. J., Kupfersberger, H., Kværner, J., Muotka, T.,
746 et al. (2014) Climate change impacts on groundwater and dependent ecosystems. *J. Hydrol.*
747 **518**(PB), 250–266. doi:10.1016/j.jhydrol.2013.06.037
- 748 Lesser, J. M. (1976) Resumen del estudio Geohidrologico e hidrogeoquimico de la península de
749 Yucatán. *Boletín Divulg. Tec.* Retrieved from <http://www.lesser.com.mx/files/76-4-Resumen-Estudio-Geohidrologico-Yucatan.pdf>

- 752 Li, Z., Liu, W. Z., Zhang, X. C. & Zheng, F. L. (2009) Impacts of land use change and climate
753 variability on hydrology in an agricultural catchment on the Loess Plateau of China. *J.
754 Hydrol.* **377**(1–2), 35–42. Elsevier B.V. doi:10.1016/j.jhydrol.2009.08.007
- 755 Liverman, D. M. & O'Brien, K. L. (1991) Global warming and climate change in Mexico. *Glob.
756 Environ. Chang. December*, 351–364.
- 757 Lloyd, J. W., Drennan, D. S. H. & Bennell, B. M. U. (1966) A Ground-Water Recharge Study in
758 North Eastern Jordan. *Proc. Inst. Civ. Eng.* **35**(4), 615–631. doi:10.1680/iicep.1966.8603
- 759 Lu, G. Y. & Wong, D. W. (2008) An adaptive inverse-distance weighting spatial interpolation
760 technique. *Comput. Geosci.* **34**(9), 1044–1055. Pergamon.
761 doi:10.1016/J.CAGEO.2007.07.010
- 762 Madsen, H., Lawrence, D., Lang, M., Martinkova, M. & Kjeldsen, T. R. (2014) Review of trend
763 analysis and climate change projections of extreme precipitation and floods in Europe. *J.
764 Hydrol.* **519**(PD), 3634–3650. Elsevier B.V. doi:10.1016/j.jhydrol.2014.11.003
- 765 Magaña, V., Amador, J. A., Medina, S., Magaña, V., Amador, J. A. & Medina, S. (1999) The
766 Midsummer Drought over Mexico and Central America. *J. Clim.* **12**(6), 1577–1588.
767 doi:10.1175/1520-0442(1999)012<1577:TMDOMA>2.0.CO;2
- 768 Marin, L. E. & Perry, E. C. (1994) The hydrogeology and contamination potential of
769 northwestern Yucatán, Mexico. *Geofísica Int.* **4**, 619–623.
- 770 Matonse, A. H., Zion, M. S., Schneiderman, E. M., Frei, A., Pierson, D. C., Anandhi, A. &
771 Lounsbury, D. (2011) Examination of change factor methodologies for climate change
772 impact assessment. *Water Resour. Res.* **47**(3). doi:10.1029/2010wr009104
- 773 McCabe, G. J. & Markstrom, S. L. (2007) A Monthly Water-Balance Model Driven By a
774 Graphical User Interface. *U.S. Geol. Surv. Open-File Rep. 2007-1088* 6. Retrieved from
775 https://pubs.usgs.gov/of/2007/1088/pdf/of07-1088_508.pdf
- 776 Meehl, G. A., Goddard, L., Murphy, J., Stouffer, R. J., Boer, G. J., Danabasoglu, G., Dixon, K.,
777 et al. (2009) Decadal predictionCan It Be Skillful? *Bull. Am. Meteorol. Soc.* **90**(10), 1467–
778 1486. doi:10.1175/2009BAMS2778.I
- 779 Meixner, T., Manning, A. H., Stonestrom, D. A., Allen, D. M., Ajami, H., Blasch, K. W.,
780 Brookfield, A. E., et al. (2016) Implications of projected climate change for groundwater
781 recharge in the western United States. *J. Hydrol.* **534**, 124–138. Elsevier.
782 doi:10.1016/J.JHYDROL.2015.12.027

- 783 Messina, M. G. & Conner, W. H. (1998) *Southern forested wetlands : ecology and management.*
784 Lewis Publishers.
- 785 Milly, P. C. D., Dunne, K. A. & Vecchia, A. V. (2005) Global pattern of trends in streamflow
786 and water availability in a changing climate. *Nature* **438**(7066), 347–350.
787 doi:10.1038/nature04312
- 788 Moss, R., Babiker, M., Brinkman, S., Calvo, E., Carter, T., Edmonds, J., Elgizouli, I., et al.
789 (2007) *Towards New Scenarios for Analysis of Emissions, Climate Change, Impacts, and*
790 *Response Strategies. Intergov. Panel Clim. Chang.* Noordwijkerhout, The Netherlands.
791 doi:10.1086/652242
- 792 Mulholland, P. J., Best, G. R., Coutant, C. C., Hornberger, G. M., Meyer, J. L., Robinson, P. J.,
793 Stenberg, J. R., et al. (1997) Effects of climate change on freshwater ecosystems of the
794 south-eastern United States and the Gulf Coast of Mexico. *Hydrol. Process.* **11**(8), 949–
795 970. doi:10.1002/(SICI)1099-1085(19970630)11:8<949::AID-HYP513>3.0.CO;2-G
- 796 Neuman, B. R. & Rahbek, M. L. (2007) Modeling the Groundwater Catchment of the Sian Ka'an
797 Reserve, Quintana Roo. Austin: AMCS Bulletin 18. Association for Mexican cave studies.
798 Retrieved from <http://www.mexicancaves.org/bul/bul18.html>
- 799 Null, K. a., Knee, K. L., Crook, E. D., Sieyes, N. R. de, Rebolledo-Vieyra, M., Hernández-
800 Terrones, L. & Paytan, A. (2014) Composition and fluxes of submarine groundwater along
801 the Caribbean coast of the Yucatan Peninsula. *Cont. Shelf Res.* **77**, 38–50. Elsevier.
802 doi:10.1016/j.csr.2014.01.011
- 803 Orellana, R., Espadas, C., Conde, C. & Gay, C. (2009) *Atlas. Escenario de cambio climático en*
804 *la península de Yucatán.* Mérida, Yucatán: CICY.
- 805 Pérez Ceballos, R. & Pacheco Ávila, J. (2004) Vulnerabilidad del agua subterránea a la
806 contaminación de nitratos en el estado de Yucatán. *Rev. UADY Ing.* **8–1**, 33–42. Retrieved
807 from <http://www.revista.ingenieria.uady.mx/volumen8/vulnerabilidad.pdf>
- 808 Ponce, V. M. (1989) Basic hydrologic principles. In: *Engineering Hydrology: Principles and*
809 *Practices*, 48–51. Retrieved from <http://onlinecalc.sdsu.edu/onlineblaneycriddle.php>
- 810 Pulido-Velazquez, D., Collados-Lara, A. J. & Alcalá, F. J. (2018) Assessing impacts of future
811 potential climate change scenarios on aquifer recharge in continental Spain. *J. Hydrol.* **567**,
812 803–819. Elsevier B.V. doi:10.1016/j.jhydrol.2017.10.077
- 813 Pulido-Velazquez, D., Renau-Pruñonosa, A., Llopis-Albert, C., Morell, I., Collados-Lara, A. J.,

- 814 Senent-Aparicio, J. & Baena-Ruiz, L. (2018) Integrated assessment of future potential
815 global change scenarios and their hydrological impacts in coastal aquifers - A new tool to
816 analyse management alternatives in the Plana Oropesa-Torreblanca aquifer. *Hydrol. Earth*
817 *Syst. Sci.* **22**(5), 3053–3074. doi:10.5194/hess-22-3053-2018
- 818 Rodríguez-Huerta, E. (2018) Variation of groundwater recharge in the Yucatan peninsula caused
819 by climate change. Retrieved from
820 <https://public.tableau.com/profile/edgar.rodriguez.huerta#!/vizhome/GroundwaterrechargeYucatanPeninsula/VIZ>
- 822 Rodríguez-Iturbe, I. (2000) Ecohydrology : A hydrologic perspective of climate-soil-vegetation
823 dynamics. *Water Resour. Res.* **36**(1), 3–9.
- 824 Rushton, K. R. (1988) Groundwater recharge estimation (Part 2): numerical modelling
825 techniques. In: *Estimation of Natural Groundwater Recharge*, 223–239. Reidel Publishing
826 Company. doi:10.1007/978-94-015-7780-9_3
- 827 Rushton, K. R. & Ward, C. (1979) The estimation of groundwater recharge. *J. Hydrol.* **41**(3–4),
828 345–361. doi:10.1016/0022-1694(79)90070-2
- 829 Sánchez Aguilar, R. L. & Rebollar Domínguez, S. (1999) Deforestación en la Península de
830 Yucatán, los retos que enfrentar. *Madera y Bosques* **5**(2), 3. doi:10.21829/myb.1999.521344
- 831 Savenije, H. H. G., Hoekstra, A. Y. & Zaag, P. Van Der. (2014) Evolving water science in the
832 Anthropocene. *Hydrol. Earth Syst. Sci.* **18**(1), 319–332. doi:10.5194/hess-18-319-2014
- 833 Saxton, K. E. & Rawls, W. J. (1986) Estimating Generalized Soil-water Characteristics from
834 Texture. *Soil Sci. Soc. Am.* 1031–1036.
- 835 Schär, C., Vidale, P. L., Lüthi, D., Frei, C., Häberli, C., Liniger, M. A. & Appenzeller, C. (2004)
836 The role of increasing temperature variability in European summer heatwaves. *Nature*
837 **427**(6972), 332–336. Nature Publishing Group. doi:10.1038/nature02300
- 838 Schulz, C. J. & García, R. F. (2015) Balance hídrico y recarga de acuíferos. Salta: Asociación
839 Interacional de hidrogeólogos. Grupo Chileno. Retrieved from http://aih-cl.org/cursos/Balance_y_Recarga_de_Acuiferos_Version_Final.pdf
- 841 SEMARNAT. (2015) Descripción del subsistema natural. In: *Bitacora de ordenamiento
842 ambiental*. Mérida. Retrieved from
843 <http://bitacoraordenamiento.yucatan.gob.mx/archivos/200605025953.pdf>

- 844 Shnerb, N. M., Sarah, P., Lavee, H. & Solomon, S. (2003) Reactive Glass and Vegetation
845 Patterns. *Phys. Rev. Lett.* **90**(3), 4. doi:10.1103/PhysRevLett.90.038101
- 846 Smerdon, B. D. (2017) A synopsis of climate change effects on groundwater recharge. *J. Hydrol.*
847 **555**, 125–128. Elsevier B.V. doi:10.1016/j.jhydrol.2017.09.047
- 848 Solé, R. V. (2011) *Phase Transitions*. New Jersey: Princeton Univeristy Press.
- 849 Storch, H. von, Zorita, E. & Cubasch, U. (1993) Downscaling of Global Climate Change
850 Estimates to Regional Scales: An Application to Iberian Rainfall in Wintertime. *J. Clim.*
851 **6**(6), 1161–1171. doi:10.1175/1520-0442 (1993)
- 852 Taylor, K. E. (2007) CMIP5: models design **2009**(January 2011), 1–33.
- 853 Taylor, K. E., Stouffer, R. J. & Meehl, G. A. (2012) An Overview of CMIP5 and Experimental
854 Design. *Bull. Am. Meteorol. Soc.* **93**(april), 485–498. doi:10.1175/BAMS-D-11-00094
- 855 Taylor, R. G., Scanlon, B., Döll, P., Rodell, M., Beek, R. Van, Wada, Y., Longuevergne, L., et
856 al. (2013) Ground water and climate change. *Nat. Clim. Chang.* **3**(4), 322–329.
857 doi:10.1038/nclimate1744
- 858 Thornthwaite, C. W. (1948) An Approach toward a Rational Classification of Climate. *Geogr.
859 Rev.* **38**(1), 55–94. Retrieved from <http://links.jstor.org/sici?doi=0016-7428%28194801%2938%3A1%3C55%3AAATARC%3E2.0.CO%3B2-O>
- 860
- 861 Thornthwaite, C. W. & Mather, J. R. (1955) The water balance. *Publ. Climatol.* **8**(1), 1–104.
- 862 Thornthwaite, C. W. & Mather, J. R. (1957) Instructions and Tables for Computing Potential
863 Evapotranspiration and Water Balance. *Publ.Climatol* **10** (3), 185–311.
- 864 Torres, M. C., Basulto, Y. Y., Cortés, J., García, K., Koh, A., Puerto, F. & Pacheco, J. (2014)
865 Evaluación de la vulnerabilidad y el riesgo de contaminación del agua subterránea en
866 Yucatán. *Ecosistemas y Recur. Agropecu.* **1**(3), 189–203.
- 867 Trenberth, K. E. (2011) Changes in precipitation with climate change. *Clim. Res.* Inter-Research
868 Science Center. doi:10.2307/24872346
- 869 USDA Natural Resources Conservation Service. (1998) Soil Quality Resource Concerns:
870 Available Water Capacity. *Soil Qual. Inf. Sheet*. Retrieved from
871 https://www.nrcs.usda.gov/Internet/FSE_DOCUMENTS/nrcs142p2_051279.pdf
- 872 Valle-Levinson, A., Mariño-Tapia, I., Enriquez, C. & Waterhouse, A. F. (2011) Tidal variability
873 of salinity and velocity fields related to intense point-source submarine groundwater

874 discharges into the Coastal Ocean. *Limnol. Oceanogr.* **56**(4), 1213–1224.
875 doi:10.4319/lo.2011.56.4.1213

876 Villasuso, M. & Méndez, R. (2000) A Conceptual Model of the Aquifer of the Yucatan
877 Peninsula: From Ancient Maya to 2030. In: *Population, Development, and Environment on*
878 *the Yucatan Peninsula* (W. Lutz, L. Prieto & W. Sanderson, eds.), 120–139. Vienna.

879 Vries, J. J. de & Simmers, I. (2002) Groundwater recharge: An overview of process and
880 challenges. *Hydrogeol. J.* **10**(1), 5–17. doi:10.1007/s10040-001-0171-7

881 Wilby, R. L., Charles, S. P., Zorita, E., Timbal, B., Whetton, P. & Mearns, L. O. (2004)
882 Guidelines for use of climate scenarios developed from statistical downscaling methods.
883 Supporting material of the Intergovernmental Panel on Climate Change, prepared on behalf
884 of Task Group on Data and Scenario Support for Impacts and Climate Analysis (August),
885 1–27. Retrieved from http://www.ctn.etsmtl.ca/cours/mgc921/dgm_no2_v1_09_2004.pdf

886 Zhou, G., Wei, X., Chen, X., Zhou, P., Liu, X., Xiao, Y., Sun, G., et al. (2015) Global pattern for
887 the effect of climate and land cover on water yield. *Nat. Commun.* **6**, 1–9. Nature Publishing
888 Group. doi:10.1038/ncomms6918

889

890 **7. Supplementary information**

891 S.I. Table 1. Land uses are grouped according to the ranges of the maximum root depth

CODE	Description (in Spanish)	Vegetation root depth category
10101010304	Agricultura de temporal permanente	Moderate
10101040102	Agricultura de temporal anual y semipermanente	Moderate
10101040103	Agricultura de temporal anual y permanente	Moderate
10101040104	Agricultura de temporal anual	Moderate
10101040203	Agricultura de temporal semipermanente y permanente	Moderate
10101040204	Agricultura de temporal semipermanente	Moderate
10102010304	Agricultura de riego permanente	Moderate
10102040102	Agricultura de riego anual y semipermanente	Moderate
10102040103	Agricultura de riego anual y permanente	Moderate
10102040104	Agricultura de riego anual	Moderate
10102040203	Agricultura de riego semipermanente y permanente	Moderate

10102040204	Agricultura de riego semipermanente	Moderate
10103040102	Agricultura de humedad anual y semipermanente	Moderate
10103040103	Agricultura de humedad anual y permanente	Moderate
10103040104	Agricultura de humedad anual	Moderate
10201040304	Pastizal cultivado	Deep
10301030304	Bosque cultivado	Orchard
10401040000	Acuícola	Moderate
20201010500	Vegetación secundaria arbórea de bosque de encino	Orchard
20201020600	Vegetación secundaria arbustiva de bosque de encino	Orchard
20401010400	Selva alta perennifolia	Mature forest
20401020500	Vegetación secundaria arbórea de selva alta perennifolia	Orchard
20401020600	Vegetación secundaria arbustiva de selva alta perennifolia	Orchard
20402010400	Selva alta subperennifolia	Mature forest
20402020400	Vegetación secundaria herbácea de selva alta subperennifolia	Orchard
20402020500	Vegetación secundaria arbórea de selva alta subperennifolia	Orchard
20402020600	Vegetación secundaria arbustiva de selva alta subperennifolia	Orchard
20404010400	Selva mediana subperennifolia	Mature forest
20404020500	Vegetación secundaria arbórea de selva mediana subperennifolia	Orchard
20404020600	Vegetación secundaria arbustiva de selva mediana subperennifolia	Orchard
20404020700	Vegetación secundaria herbácea de selva mediana subperennifolia	Orchard
20405010400	Selva baja perennifolia	Orchard
20406010400	Selva baja subperennifolia	Orchard
20406020500	Vegetación secundaria arbórea de selva baja subperennifolia	Deep
20501010400	Selva mediana subcaducifolia	Orchard
20501020500	Vegetación secundaria arbórea de selva mediana subcaducifolia	Orchard
20501020600	Vegetación secundaria arbustiva de selva mediana subcaducifolia	Orchard
20501020700	Vegetación secundaria herbácea de selva mediana subcaducifolia	Orchard
20502010400	Selva baja subcaducifolia	Orchard
20502020500	Vegetación secundaria arbórea de selva baja subcaducifolia	Deep
20502020600	Vegetación secundaria arbustiva de selva baja subcaducifolia	Deep
20601010400	Selva mediana caducifolia	Mature forest
20601020500	Vegetación secundaria arbórea de selva mediana caducifolia	Orchard
20601020600	Vegetación secundaria arbustiva de selva mediana caducifolia	Orchard

20601020700	Vegetación secundaria herbácea de selva mediana caducifolia	Orchard
20602010400	Selva baja caducifolia	Orchard
20602020500	Vegetación secundaria arbórea de selva baja caducifolia	Deep
20602020600	Vegetación secundaria arbustiva de selva baja caducifolia	Deep
20602020700	Vegetación secundaria herbácea de selva baja caducifolia	Deep
20701020500	Vegetación secundaria arbórea de selva baja espinosa caducifolia	Deep
20701020600	Vegetación secundaria arbustiva de selva baja espinosa caducifolia	Deep
20702010400	Selva baja espinosa subperennifolia	Deep
20702020500	Vegetación secundaria arbórea de selva baja espinosa subperennifolia	Deep
20702020600	Vegetación secundaria arbustiva de selva baja espinosa subperennifolia	Deep
20702020700	Vegetación secundaria herbácea de selva baja espinosa subperennifolia	Deep
20802010400	Pastizal halófilo	Deep
20807010400	Sabana	Deep
21001020500	Vegetación secundaria arbórea de selva de galería	Orchard
21003010400	Manglar	Moderate
21003020500	Vegetación secundaria arbórea de manglar	Orchard
21003020600	Vegetación secundaria arbustiva de manglar	Orchard
21006030400	Popal	Deep
21007030400	Tular	Deep
21008010400	Vegetación de petén	Deep
21008020500	Vegetación secundaria arbórea de vegetación de petén	Deep
21009010400	Vegetación halófila hidrófila	Moderate
21102010400	Vegetación de dunas costeras	Moderate
21103010400	Palmar natural	Deep
21201030300	Sin vegetación aparente	Shallow
21301030300	Palmar inducido	Deep
21302030300	Pastizal inducido	Deep
30000000030	Desprovisto de vegetación	Shallow
30000000031	Cuerpo de agua	None
30000000032	Asentamientos humanos	Moderate
30000000033	Zona urbana	Moderate

892 ***7.1. Data Availability***

893 In order to facilitate the model reproduction and apply under different climate change scenarios,
894 the R code is attached in the following link –expecting it will serve as a support for the different
895 hydrological studies that are being developed in the region–.

896 <https://summlabbd.upc.edu/rodriguez-huerta-et-al/>